METAL OXIDATION LASER

Leslie G. Murray

NPS-57Co74061

NAVAL POSTGRADUATE SCHOOL
Monterey, California

THESIS

METAL OXIDATION LASER

Leslie G. Murray

June 1974

Thesis Advisor: J. D. Collins

J. Willis Code 310A
Naval Air Systems Command
Washington, D.C. 20360

SECURITY CLASSIFICATION OF THIS PAGE (When Data Entered)

REPORT DOCUMENTATION PAGE		READ INSTRUCTIONS BEFORE COMPLETING FORM
1. REPORT NUMBER	2. GOVT ACCESSION NO.	3. RECIPIENT'S CATALOG NUMBER
4. TITLE (and Subtitle) Metal Oxidation Laser		5. TYPE OF REPORT & PERIOD COVERED Master's Thesis; June 1974 6. PERFORMING ORG. REPORT NUMBER
7. AUTHOR(s) Leslie G. Murray		8. CONTRACT OR GRANT NUMBER(s)
9. PERFORMING ORGANIZATION NAME AND ADDRESS Naval Postgraduate School Monterey, California 93940		10. PROGRAM ELEMENT, PROJECT, TASK AREA & WORK UNIT NUMBERS
11. CONTROLLING OFFICE NAME AND ADDRESS Naval Postgraduate School Monterey, California 93940		12. REPORT DATE June 1974 13. NUMBER OF PAGES 74
14. MONITORING AGENCY NAME & ADDRESS(if different from Controlling Office) Naval Postgraduate School Monterey, California 93940		15. SECURITY CLASS. (of this report) Unclassified 15a. DECLASSIFICATION/DOWNGRADING SCHEDULE

16. DISTRIBUTION STATEMENT (of this Report)

Approved for public release; distribution unlimited

17. DISTRIBUTION STATEMENT (of the abstract entered in Block 20, if different from Report)

18. SUPPLEMENTARY NOTES

19. KEY WORDS (Continue on reverse side if necessary and identify by block number)

20. ABSTRACT (Continue on reverse side if necessary and identify by block number)

The work reported in this thesis consisted of two parts: (1) experiments with a CO_2-CH_3N_3 laser system previously constructed, and (2) the design and construction of a metal oxide laser system.

The experiments with the CO_2-CH_3N_3 laser were to determine if a chemical laser is feasible utilizing a pumping scheme where energy released by photolysis of CH_3N_3 is used to create a population inversion in CO_2. Lasing action

DD FORM 1 JAN 73 1473 (Page 1) EDITION OF 1 NOV 65 IS OBSOLETE S/N 0102-014-6601 |

SECURITY CLASSIFICATION OF THIS PAGE (When Data Entered)

20. (cont'd)

was not obtained because the chemical process utilized to prepare CH_3N_3 did not produce enough CH_3N_3 gas to carry out the experiments.

A metal oxide laser system was designed and constructed. The energy from an exothermic chemical reaction between a metal and an oxidizing gas was utilized to create a population inversion in the diatomic product molecules. The metal was vaporized using the exploding wire technique. The laser tube, resonant cavity, vacuum system, electrical control system and exploding wire circuit were designed and fabricated. Several experiments were performed using aluminum, copper and indium wire with oxygen gas. No lasing action was observed in the case of aluminum and copper oxide; indium oxide appeared to lase, but more experiments will be required to confirm lasing in the indium oxide molecule.

METAL OXIDATION LASER

by

Leslie G. Murray
Lieutenant, United States Navy
B.S., University of Idaho, 1968

Submitted in partial fulfillment of the
requirements for the degree of

MASTER OF SCIENCE IN AERONAUTICAL ENGINEERING

from the

NAVAL POSTGRADUATE SCHOOL
June 1974

ABSTRACT

The work reported in this thesis consisted of two parts: (1) experiments with a CO_2-CH_3N_3 laser system previously constructed, and (2) the design and construction of a metal oxide laser system.

The experiments with the CO_2-CH_3N_3 laser were to determine if a chemical laser is feasible utilizing a pumping scheme where energy released by photolysis of CH_3N_3 is used to create a population inversion in CO_2. Lasing action was not obtained because the chemical process utilized to prepare CH_3N_3 did not produce enough CH_3N_3 gas to carry out the experiments.

A metal oxide laser system was designed and constructed. The energy from an exothermic chemical reaction between a metal and an oxidizing gas was utilized to create a population inversion in the diatomic product molecules. The metal was vaporized using the exploding wire technique. The laser tube, resonant cavity, vacuum system, electrical control system and exploding wire circuit were designed and fabricated. Several experiments were performed using aluminum, copper and indium wire with oxygen gas. No lasing action was observed in the case of aluminum and copper oxide; indium oxide appeared to lase, but more experiments will be required to confirm lasing in the indium oxide molecule.

TABLE OF CONTENTS

LIST OF FIGURES

I. INTRODUCTION

The body of knowledge that comprises the laser field has grown at a rate rarely experienced in science. Beginning with the first pulse of coherent emission from single crystalline ruby by Maiman in 1960, the laser field today draws from numerous disciplines: physics, optics, electronics, organic and inorganic chemistry, kinetics, fluid dynamics, aerodynamics, and crystallography. The laser research in progress today is demanding of our present engineering technology.

Historically, the ever increasing demands for communication have sparked man's drive toward the production and use of coherent electromagnetic energy of shorter and shorter wave length. An added incentive was the use of such radiation as a research tool for probing the secrets of the atom by techniques such as paramagnetic resonance and cyclotron resonance. Today the laser is used in holography, optical ranging, extremely high resolution spectroscopy and many other applications.

Light is an electromagnetic wave which can be expressed by the wave function Ψ which describes its propagation:

$$\Psi = \Psi(x, y, z) \exp(-2\pi i \nu t + i\phi)$$

ϕ is the phase angle and ν is the frequency. Waves which have the same direction, phase angle and frequency are coherent. Coherent radiation has a much greater intensity than incoherent radiation which, in communications for example, translates into a much greater range. The higher the frequency of the carrier wave, the greater the information carrying capacity, directivity and efficiency available. The quest for higher and higher coherent sources of electromagnetic radiation has progressed from vacuum tube oscillators to today's lasers in the visible region and is expanding towards devices in the far ultraviolet and soft x-ray region.

The theory leading to the discovery of lasers began in 1916 when Einstein showed that stimulated emission of light from an excited atom could be obtained when the Bohr frequency condition is satisfied for some pair of levels and that the stimulated radiation was in phase with the stimulating radiation. During the 1920's and 1930's much work was done exploring the consequences of the Fuchtbauer-Ladenburg formula which linked the absorption coefficient of material with the Einstein coefficients of its constituent molecules and the distribution of these molecules among the different energy levels.

World War II proved a great stimulus to science in general; many scientific experiments were performed which made use of the interaction of microwaves with matter. The idea of "population inversion" was advanced by Fabrikant and was manifested in the experiments of Block, Hansen, and Packard in 1946 and Lamband Retherford in 1950. In 1951 Percell and Pound obtained evidence of stimulated emission of a 50 KHz signal from a nuclear spin system.

In 1952 the "Quarterly Reports of Columbia Radiation Laboratory" began publishing summaries of the progress of an ammonia maser under construction. Late in 1953, Townes and two of his students, Gordon and Zeiger, succeeded in operation of the ammonia maser. In 1954 Basov and Prokhorov of the Lebdev Institute, Moscow, independently of Townes, published an article containing a detailed theoretical exploration of the use of microwave spectroscopy and detailed calculations pertaining to the role of the relevant physical parameters of a similar ammonia maser.

The remaining years of the fifties were given over to searching for masers at higher and higher frequencies. 1957 and 1958 saw the development of the ruby maser and its application to radio astronomy and radar. In 1958 Townes and Schawlow published the article which summarized the

challenge, the rewards and the difficulties in extending stimulated emission techniques to the infrared and optical region of the spectrum. Most of the efforts towards producing a visible maser were concentrated in the area of optically excited alkali vapors and noble gases excited by an electric charge.

In July, 1960, Maiman, then at the Hughes Aircraft Company, invented the ruby laser; his achievement came as a surprise, although it was not an accidental discovery. In the fall of 1960 Javan at the Bell Telephone Laboratories announced the expected successful operation of the He-Ne laser. The end of 1960 saw the discovery of three new solid lasers and a feverish race between half a dozen laboratories pushing their laser work to completion.

Early in 1964, Patel reported the observation of CW laser action in CO_2 gas at 10.6 microns. Although this discovery did not attract any more attention than hundreds of other laser transitions being reported at the time, by 1966 it was evident that the efficiency and average output power of this laser were unique when compared with all other existing lasers. Since 1964 much work has been done to develop the CO_2 laser and to develop new lasers with specific output power and small size and weight.

The work reported herein is composed of two parts: (1) experiments with a chemically pumped gas laser which is a variation of the basic CO_2 laser; and (2) design, construction and preliminary experiments with a metal oxide laser.

To gain experience and expertise in gas and chemical laser systems, several preliminary experiments were performed using a CO_2-HN_3 laser system designed and fabricated in previous thesis work [Ref. 16]. The problems of aligning the optics associated with a laser system were thoroughly

explored. The system was slightly modified to accommodate the nature of the experiments and some of the equipment was replaced or repaired.

The experiments studied the lasing possibilities of a chemically pumped CO_2 laser. Photolysis of methyl azide (CH_3N_3) was used to produce excited N_2 molecules which created a population inversion in the CO_2 by resonance transfer. The results of these experiments are given in Section II.

The bulk of the work undertaken was to design and construct a metal oxide laser system. The system involves a vacuum system, gas handling system, high voltage capacitor bank and power supply, and necessary electronic equipment for firing and monitoring the output of the system.

The laser tube, optical cavity, detectors and filters and most of the vacuum system plumbing is located in a plexiglass enclosure. Particularly troublesome during construction was the vacuum system; the large number of fittings and valves contributed to the leakage problem.

Several experiments with different metals were conducted to determine current and voltage characteristics of the exploding wire phenomenon. Experiments were also conducted to determine the lasing characteristics of different metal oxides. One objective was to reproduce results obtained by Jensen and Rice at Los Alamos [Ref. 12]. Results of these experiments are described in Section III. The purpose of this work was to produce a research tool to further explore the possibilities of a visible chemical laser utilizing oxides, halides and fluorides of metals, particularly of the rare earths.

II. THE CH_3N_3 LASER

A. GENERAL

The equipment used in the CH_3N_3 laser experiments was designed and constructed by LCDR G. P. Schnez, Federal German Navy, and is described in Ref. 16. The system was designed as a variation of a basic CO_2-N_2 laser and is pulsed rather than CW operated. The experiments conducted by Schnez, and later by ENS T. L. Houck [Ref. 5], involved a CO_2 laser chemically pumped by photolysis of hydrogen azide (HN_3). Several modifications have been made to the system, the most important being installation of a more accurate pressure monitoring equipment. The modifications are detailed in the following section describing the equipment and experimental procedure.

In the past ten years, the CO_2 laser has been extensively studied and the theory is well known; Ref. 8 gives a very complete coverage of the CO_2 laser. The CO_2-CH_3N_3 laser system examined in these experiments is a CO_2 gas laser that is chemically pumped by photolysis of CH_3N_3. Dzhidzhoev in Ref. 3 gives a good description of chemical pumping. Chemical pumping is an attempt to improve the laser efficiency over the classical electric discharge method of pumping a CO_2 laser.

B. CO_2-CH_3N_3 LASER CHEMISTRY

In a CO_2-N_2 laser, the upper lasing level of CO_2 is pumped predominantly by vibrational energy transfer from excited N_2. A pumping scheme which would raise a large fraction of N_2 molecules to an excited energy level would greatly increase the laser efficiency. Dzhidzhoev [Ref. 3] has reported chemical pumping of N_2 by flash photolysis of a mixture of

HN_3 (hydrazoic acid) and CO_2. A laser system utilizing photolysis of HN_3 in CO_2 has been successfully operated and is summarized in Refs. 16 and 5. The goal of these experiments was to investigate a CO_2 laser chemically pumped by flash photolysis of methyl azide (CH_3N_3).

The products of the flash photolysis of CH_3N_3 are predominantly N_2, with small amounts of H_2, CH_4, C_2H_6 and HCN. The important primary process is [Ref. 1]:

$$CH_3N_3 + h\nu \longrightarrow CH_3N + N_2 \qquad (1)$$

The small yields of CH_4, C_2H_4, C_2H_6 and HN_3 rule out the processes

$$CH_3N_3 + h\nu \longrightarrow CH_3 + N_3 \qquad (1a)$$

$$CH_3N_3 + h\nu \longrightarrow CH_2 + HN_3 \qquad (1b)$$

as being important primary reactions.

The quantum yield of N_2 is dependent upon the wave length of the incident radiation; ϕ_{N_2} ranges from 1.7 in the range 2750-3130Å to 2.3 at 2540Å. ϕ_{N_2} is also found to be essentially independent of time, intensity and temperature to 100°C at low pressures, less than 100 torr and small conversion rates [Ref. 1].

Details of the decomposition process (1) and the nature of the radical CH_3N are given as follows [Ref. 9]:

$$CH_3N_3 + h\nu \longrightarrow CH_3N(\chi^3\Sigma^-) + N_2(\chi^1\Sigma_g^+) \qquad (2a)$$
$$\Delta H = 9.5 \text{ kcal mole}^{-1}$$

$$CH_3N_3 + h\nu \longrightarrow CH_3N(a^1\Delta) + N_2(\chi^1\Sigma_g^+) \qquad (2b)$$
$$\Delta H = 46.5 \text{ kcal mole}^{-1}$$

$$CH_3N_3 + h\nu \longrightarrow CH_3N(b^1\Sigma^+) + N_2(\chi^1\Sigma_g^+) \qquad (2c)$$
$$\Delta H = 71.0 \text{ kcal mole}^{-1}$$

Since there is no information available concerning the dissociation energy of the CH_3N-N_2 bond, it is common practice to assume that the bond energy is about the same as for HN-N_2, 40.5 Kcal mole^{-1} [Refs. 1 and 9]. Much

more energy is available in the photochemical process than in the thermal process, therefore it is highly probable that processes (2b) or (2c) take place in the photolysis decomposition. Dzhidzhoev takes the excess energy as 71.0 Kcal $mole^{-1}$ for $HN-N_2$ [Ref. 3]; therefore process (2c) would appear to be what does in fact take place.

Secondary reactions in the photolysis are

$$CH_3N_3 + CH_3N \longrightarrow (CH_3N)_2 + N_2 \qquad (3)$$

$$CH_3N^* \longrightarrow H_2 + HCN \qquad (4)$$

The production of H_2 decreases with increasing pressure. The addition of CO_2 to the CH_3N_3 did not adversely affect the production of N_2. Even 120 times as much CO_2 as CH_3N_3 did not reduce the rate by more than 20% [Ref. 1].

C. CO_2-CH_3N_3 EXPERIMENTAL SETUP

1. General Description

The CO_2-CH_3N_3 laser system used in these experiments consists of a laser tube, optical cavity, gas generating and handling system, vacuum system, flashlamp and high voltage capacitor bank, and associated electronic equipment and a vacuum pump. Due to the toxic nature of the materials used in the experiments, the bulk of the laser system is located inside a fume hood exhausted to the atmosphere. During the experiments the fume hood is closed by a sliding glass window and the exhaust system keeps the interior of the hood below atmospheric pressure to prevent leakage of any gases to the room. An additional plexiglass shield was installed to protect the experimenter during the mixing of the chemicals.

The remainder of the system equipment is located outside the hood. All system valves are remotely operated from a control panel by toggle switches and the position of the valves is indicated by a red light for

each valve. The flashlamp power supply is a high voltage capacitor bank which is also used in the metal oxide laser described in Section III. The CO_2-CH_3N_3 system is shown in Figures 1 and 2.

2. Optical System

The optical system consists of the laser tube, the optical cavity and the detector and associated filters; the optical system, with the exception of the detector, is located in the fume hood. The optical system is illustrated in Figure 5. The laser tube is made of fused quartz and is 60cm long with an inside diameter of 20mm. The laser tube is closed with NaCl windows mounted at the Brewster angle, $56^{\circ}40'$. The tube is held in place by teflon clamps that are mounted on an optical bench by steel stanchions. The flashlamp tube also fits in the clamps parallel to the laser tube; the flashlamp and laser tube are surrounded by a clam-shell reflector that is attached to the steel stanchions.

The optical cavity is formed by two gold-surfaced one-inch diameter mirrors; the mirrors are spherically concave of radius 10 meters. The mirrors are placed in gimbal mounts and mounted on the optical bench 78cm apart. The end mirror, M1, has a 1mm hole in the center to couple energy out of the cavity.

3. Gas Handling and Vacuum System

The gas generating system consists of a 500-ml pyrex flask, with a teflon coated magnetic stir, a darkened 3-liter storage flask and the necessary piping to connect it to the gas handling system. The generating flask is connected to the system by two glass ball joints to facilitate removal for cleaning. All valves in the gas generating system are manually operated. The valve connecting the gas storage bottle to the gas distribution manifold is electrically operated from the remote control panel.

The vacuum and gas handling system is composed of $\frac{1}{4}$-inch stainless steel tubing, and the gas distribution manifold is made up of 1/8-inch stainless steel tubing. All system valves are solenoid actuated from a remote control panel, Figure 2. The system is connected to the laser tube by a combination of ball joints and flexible stainless steel bellows. Research grade gases to be used in the experiments are stored in one-liter pyrex flasks located outside the fume hood. Commercial grade nitrogen used to flush the system is also stored outside the hood in a metal cylinder. All gas flow rates are set by manually operated needle valves and the amount of gas in the system is determined by measurement of the partial pressures of each individual gas. The gas handling and vacuum system is shown in Figure 1.

Pressure in the system is measured with an MKS Baratron Type 170 Pressure Meter utilizing a capacitive sensor with a direct digital readout with a range of 0-100 torr. Secondary pressure measurement is provided by a stainless steel Bourdon tube gauge with a range of 0-800mm of mercury and accuracy of 0.1% of full scale. The MKS pressure meter was used to determine the partial pressures of the components gases. An electrical driven mechanical vacuum pump is installed and can produce a vacuum of 10^{-3} torr in the system. The system was accepted with a leak rate of approximately 4 torr per hour.

4. Flashlamp and High Voltage System

The flashlamp used to effect the photolysis reaction was an ILC Model 10L24 Xenon filled flashlamp, 60cm by 10cm, with a fused-quartz tube and nickel-plated copper electrodes. The high voltage circuit to drive the flashlamp consists of a capacitor bank made up of four high voltage oil-filled capacitors of 7μf each connected in parallel, an inductance

made of 3/8-inch copper tubing with 25 windings and a diameter of 15cm and a trigger network. The high voltage system is described in detail in Ref. 16.

The high voltage charging control system and the trigger circuit are the same equipment used for the metal oxide laser and its operation is described in Section III.D.5. The amount of capacitance was increased to 28μf and the bank was connected directly to the flashlamp in series with the inductance with 3/8-inch copper tubing. The total inductance in the circuit is 30μH, which is required to get the desired pulse duration from the flashlamp.

5. Electrical System

The electrical system consists of an isolation power transformer for the electronic equipment and a remote control panel, Figure 2, for the system valves. All of the valves in the vacuum and gas handling system are solenoid-actuated, electrically operated valves. Each valve is operated by a toggle switch and has a red light to indicate its condition: light on--valve open; light off-valve shut. The control panel has a relay circuit wired in to test the lights. The top of the control panel is made of plastic with a diagram of the laser system drawn on it. Each valve is represented by its light, with the toggle switch directly below the light. Remote control of the valves was necessary due to the toxic nature of the gases used in the experiments.

D. CO_2-CH_3N_3 EXPERIMENT

1. Preparation

The system is first thoroughly cleaned, paying close attention to the gas generating unit, and all ball joints and vacuum seals are coated with a thin film of vacuum grease and reassembled. The laser tube and

gas handling system is then flushed with commercial grade N_2. The optical system is now aligned following the procedure given in Appendix A.

The infrared detector is cooled to 77°K with liquid N_2 and positioned in place, Figure 5. A Tektronic Type 549 storage oscilloscope is used to monitor the output of the IR detector. An Irtran II filter and a germanium lens, f=25mm, are used to filter out the visible light from the flashlamp from the detected signal. A photo-multiplier detects the flashlamp output and is used to trigger the oscilloscope sweep.

2. Generation of Methyl Azide

The CH_3N_3 is prepared from sodium azide (NaN_3) and $CH_3C_6H_4SO_3CH_3$.

$$NaN_3 + CH_3C_6H_4SO_3CH_3 \longrightarrow CH_3N_3 + NaC_6H_4SO_3CH_3 \qquad (5)$$

The CH_3N_3 produced is in gaseous form and is passed through $CaCl_2$ to remove any moisture. Enough gas is produced at any one time to run several experiments. One gram of NaN_3 mixed with enough $CH_3C_6H_4SO_4CH_3$ to ensure complete reaction will produce 4.4 liter of CH_3N_3 at a pressure of 63.5 torr. The CH_3N_3 is stored in the gas stored flash until needed.

Operation of the gas generating system is as follows (see Figures 9 and 10 in Ref. 16):

1. Pour desired amount of NaN_3 into flask through the relief valve stop cock and replace stop cock.
2. Fill the burette above valve MV1 with the desired amount of $CH_3C_6H_4SO_3CH_3$.
3. Open valves S, T and MV3 and flush with N2.
4. With S and MV3 open, pump down entire system.
5. Open MV1 and fill the burette above MV2, close MV1.
6. Close valve S.
7. Open MV2 to add $CH_3C_6H_4SO_3CH_3$ to the NaN_3, turn on electric stirring motor.

The process (5) will take place and the CH_3N_3 is generated. The laser tube may be filled with any partial pressure of CH_3N_3 by opening and closing of S.

3. CH_3N_3 Experimental Procedure

The laser system is prepared and the CH_3N_3 gas generated as outlined in Sections II.D.1 and II.D.2 above. The laser tube is pumped down and the flashlamp is fired once without any reactants in the system to provide a base for comparison. To fire the flashlamp, the capacitor bank is charged to about 8 KV; operation of the capacitor charging system is described in Section III.C.5. The flashlamp is fired by momentarily depressing the manual trigger switch on the PG-10 pulse generator. The output of the IR detector is monitored on the storage oscilloscope.

The laser tube is now charged with CH_3N_3 gas to a pressure of about 10 torr by momentarily opening valve S. The flashlamp is again fired and the output of the IR detector monitored on the oscilloscope. The two photographs obtained are used as a base for comparison.

The laser tube is next flushed with N_2 and pumped down. The laser tube is then charged with CH_3N_3 to a pressure of about 20 torr, and an equal amount of CO_2 is added through valve C. The flashlamp is then fired and the output monitored. The experiment is repeated several times, varying the gas mixture each time to optimize the output.

E. CH_3N_3: RESULTS AND CONCLUSIONS

The major objectives of the CH_3N_3 laser experiments were to gain experience with chemical lasers and to determine if a CO_2 laser could be pumped by the photolysis of CH_3N_3. These results were not obtained from the experiments reported in this thesis.

In previously conducted gain experiments using CH_3N_3 there were indications that lasing had occurred. In this series of experiments an optical cavity was constructed and lasing, not gain, experiments were conducted. This was done because of some ambiguities in the results of the gain experiments. In the experiments reported in this thesis, a new supply of NaN_3 was used. This resulted in a considerable problem with respect to the generation of CH_3N_3.

The generation of CH_3N_3 gas from the reaction given in Equation (5) was not suffucient to enable laser experiments to be carried out. The reaction was allowed to run over a period of two hours and produced 4.4 torr of gas at a pressure of 6 torr. Several attempts using different batches of chemicals under varying conditions failed to produce a greater amount of gas.

The gain experiments and research reported in the literature indicate that a pumping scheme utilizing photolysis of CH_3N_3 may be feasible. It is recommended that (1) a method of CH_3N_3 gas preparation be found that would produce sufficient quantities of gas, and (2) that CH_3N_3 laser experiments be undertaken when a reliable gas generation method is found.

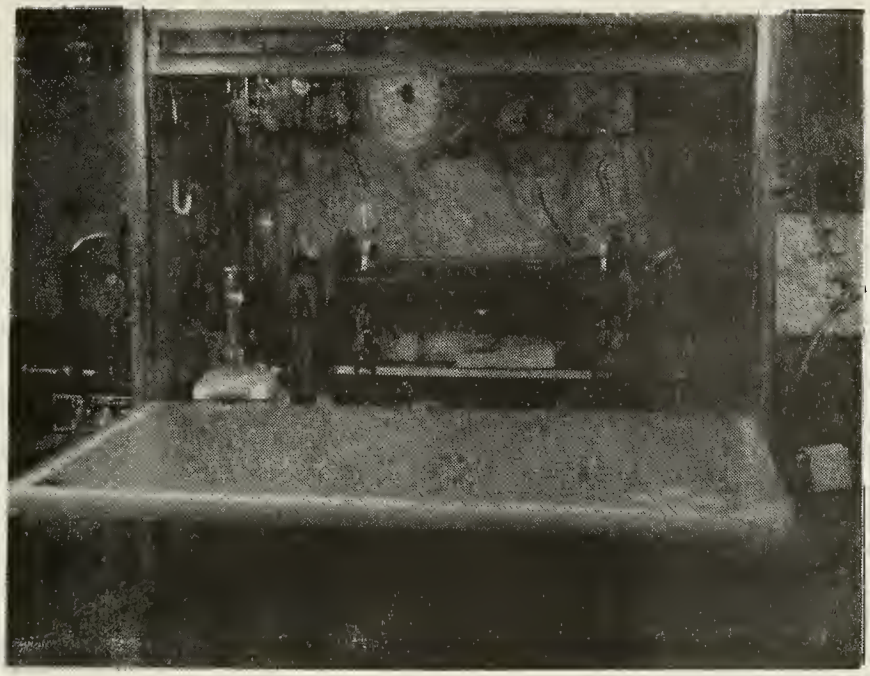

Figure 1. CO_2-CH_3N_3 Laser System

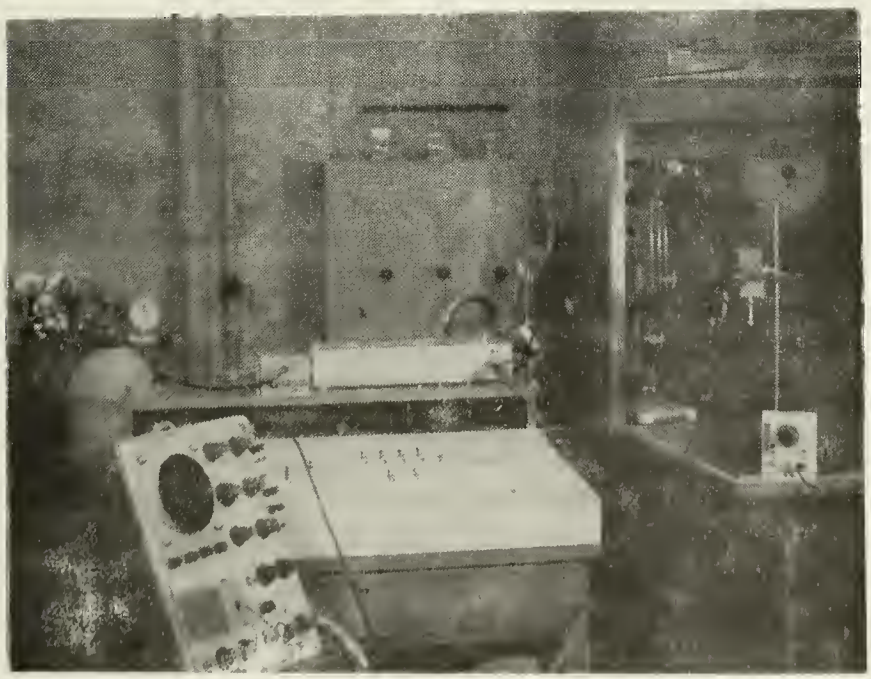

Figure 2. CO_2-CH_3N_3 Laser
Remote Control Panel and Instrumentation

III. METAL OXIDE LASER

A. BACKGROUND

The first lasers utilizing metal atoms as a lasing subject were metal-vapor lasers. A metal-vapor laser is essentially an electric discharge laser using a rarefied gas, such as helium, to carry the discharge and a metal vapor which acts as the lasing medium. The first metal-vapor laser was a cesium-vapor laser which was pumped by a helium flash lamp and had an IR output. In 1972 Klein and Silfvast developed a laser which employed selenium vapor and operated cw in a helium-selenium discharge. It produced visible laser light including blue, green, yellow, orange and red [Ref. 18].

In 1972, Russell, Nerhein and Pivirotto developed a supersonic electric-discharge copper-vapor laser. A high velocity flow was obtained by expanding a heated mixture of copper vapor, argon and helium through a supersonic nozzle. The optical cavity was formed by electrode assemblies and reflecting end mirrors with its axis transverse to the gas flow. The pulse discharge was supplied by high voltage capacitors which are discharged by a spark gap and associated triggering equipment. Visible laser output at 5106Å and 5782Å was obtained [Ref. 14].

The lasers described in the preceding paragraphs utilized electrical means to produce visible and infrared emission from electronic transitions. Electrically pumping a laser system often entails large and complex power supplies while chemical pumping offers the potential means for utilization of economical and convenient energy sources. A hybrid scheme using a combination of electrical and chemical pumping could require a minimum of electrical input energy.

A committee on new gas visible lasers, during a 3-day meeting in September, 1972, proposed several approaches to be utilized in obtaining a visible gas laser. One recommendation was to utilize the chemical energy from metal oxidation reactions to pump a laser. The committee's report is given in Ref. 15. Other work done to date on metal oxides is given in Ref. 12.

B. CHEMICAL LASERS

Chemical lasers differ from other lasers in the manner in which the population inversion is obtained. The general principles of laser theory are well known and will not be repeated here. Excellent discussions on specific laser systems are given in References 7 and 8. Chemical lasers are quite often hybrid systems in which the lasing medium may be a gas or mixture of gases and some means of initiating the laser-producing chemical reaction. Only a summary of chemical laser principles will be presented.

Of particular interest here is a laser in which the active medium is a gas and metallic vapor mixture in which a chemical reaction is taking place. The active medium needs to provide the optical amplification necessary for laser action. If the laser system is treated as an oscillator, with several modes, then the energy condition for gain is that a net excess of stimulated emission plus spontaneous emission exist in the active medium over the rate at which photons are lost from one oscillator mode.

The expression for the absorption coefficient α_o at the center of a transition, for which the natural broadening is neglected, is [Ref. 7]

$$\alpha_o = \frac{2\sqrt{\pi \ln 2}\ (e^2/mc)}{\Delta \nu_o} f_{21}\left(N_1 - \frac{g_1}{g_2} N_2\right) \qquad (6)$$

Where

e = electron charge

m = electron mass

c = velocity of light

f_{21} = oscillator strength of transition from state 2 to state 1

N_1 = population density in lower laser level (state 1)

N_2 = population density in upper laser level (state 2)

g_1, g_2 = statistical weights of state 1 and state 2

$\Delta\nu_D$ = Doppler width of the transition given by

$$\Delta\nu_D = \frac{2\nu_o}{c}\sqrt{\frac{2kT}{M}\ln 2} \tag{7}$$

Where

ν_o = center frequency of transition

k = Boltzmann constant

T = absolute temperature

M = atomic mass

The absorption coefficient at a frequency ν_1 is given by

$$\alpha_1 = \alpha_o \exp\left\{-\left[\frac{2(\nu_1 - \nu_o)}{\Delta\nu_D}\sqrt{\ln 2}\right]^2\right\} \tag{8}$$

A Boltzmann distribution in which the population density of lower state exceeds that of upper state is the case in all media under thermal equilibrium. In certain cases, such as a gaseous discharge under nonequilibrium conditions, it is possible to have a population inversion resulting in negative absorption or gain of electromagnetic energy propagating in the medium.

For optical gain we need

$$\frac{g_1}{g_2} N_2 > N_1 \tag{9}$$

The rate equations for states 1 and 2 are given as

$$\dot{N}_1 = n_1 - N_1/\tau_1$$

$$\dot{N}_2 = n_2 - N_2/\tau_2$$

where

n_1 = pumping rate into state 1

n_2 = pumping rate into state 2

$_1$ = effective lifetime of state 1

$_2$ = effective lifetime of state 2

Under steady state conditions we obtain

$$N_1 = n_1 \tau_1$$

$$N_2 = n_2 \tau_2$$

where

$n_1 = N_2 A_{21}$ + all other sources of atoms into state 1

A_{21} = spontaneous emission probability of transition from state 2 to 1

Thus the condition for optical gain becomes

$$n_2 \tau_2 > \frac{g_2}{g_1} n_1 \tau_1 \qquad (10)$$

Depending upon the excitation conditions, lifetime requirements are different and since the excitation rates n are often unknown, a general condition to fulfill is

$$\tau_2 \gg \frac{g_2}{g_1} \tau_1 \qquad (11)$$

In an optical oscillator, electromagnetic waves are damped by such losses as diffraction and reflections at the mirrors, and photons being scattered out of the medium due to collisions. Therefore the optical gain in a single pass through the optical medium must exceed the single pass losses; for small gain and loss

$$-\alpha l > \text{loss} \qquad (12)$$

where l is length of medium, becomes a condition for oscillation. Substituting for α_o (eq. 6) one gets

$$\frac{g_1}{g_2} n_2 \tau_2 - n_1 \tau_1 > \frac{(\text{loss})}{l} \frac{\Delta \nu_o}{2\sqrt{\pi \ln 2}\,(e^2/mc)\, f_{21}} \qquad (13)$$

Equation (13) gives the general criteria of a medium to be used to obtain laser action. The excitation rates should be such that equation (13) is satisfied in addition to the requirements of suitable lifetimes.

The preceding discussion has established the need to obtain a population inversion in a medium but has not explored the methods of doing so. Pumping by means of a chemical reaction is of interest here; the energy required to populate the upper laser level comes from the making and breaking of chemical bonds within the laser medium. As the complexity of a laser material increases, it is increasingly more difficult to selectively populate quantum levels of interest and to obtain significant energy output compared to energy input. The additional number of energy states that polyatomic molecules possess over diatomic molecules points to diatomics as candidates. The type of reaction used has to be capable of producing a population inversion; this requires a large number of excited particles, temperature as low as possible and reaction rates greater than the relaxation rates.

In the reaction

$$A + BC \longrightarrow AB^* + C \qquad (14)$$

we must make a strong A-B bond while breaking a weak B-C bond to meet the requirement of an exothermic reaction. To break the B-C bond some sort of initiation mechanism generally has to be employed. The energy available to populate the excited states is initiation energy E and the exothermicity of the reaction ΔH.

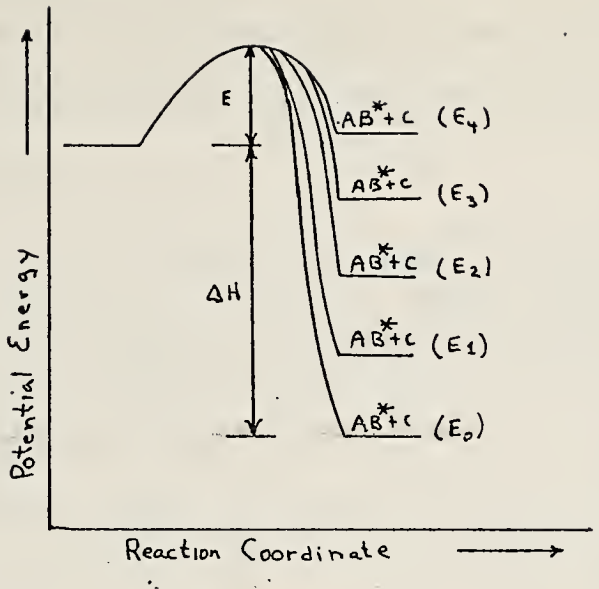

FIGURE 3

Several examples of the various types of reactions which have produced laser action are

$$H + Cl_2 \longrightarrow HCl^* + Cl$$
$$F + HBr \longrightarrow HF^* + Br$$
$$Ca + F_2 \longrightarrow CaF^* + F$$

Figure 3 depicts possible distributions of the exothermic energy from a chemical reaction. In principle, chemical laser pumping might excite electronic, vibration-rotation or pure rotational laser transitions. Electronic population inversions can be expected to be rather rare since most electronic transitions involve quite high energies relative to reaction heats. Rotational population inversions may be produced but are difficult to maintain because of the fast rotation-translation equilibrium rates. Since only moderate energies are required and many thousands of molecular collisions are required to reach vibrational equilibrium many possibilities exist for vibrational population inversions [Ref. 10].

Table I lists some of the percentages of reaction heat that can enter vibrational modes. The average percentage is likely to be much lower than

some of the high figures indicated, but Table I supports the fact that exothermic chemical reactions forming diatomic molecules deposit a large fraction of their energy in the vibrational degrees of freedom of the product molecules.

Reaction	ΔH	MAX v'	% of ΔH in vib'n mode
$D + Cl_2 \rightarrow DCl^* + Cl$	-45	2	32
$H + Cl_2 \rightarrow HCl^* + Cl$	-45	2	45
$Cl + HI \rightarrow HCl^* + I$	-32	3	70
$F + H_2 \rightarrow HF^* + H$	-32	2	80
$F + D_2 \rightarrow DF^* + D$	-32	3	85

TABLE I. Maximum observed percentage of reaction heat transferred into vibrational modes [Ref. 10].

Vibrationally and rotationally excited molecules usually radiate in the infrared or microwave region; chemical lasers produced to date involve mostly laser emission in the infrared regions. Electronic transitions involve spatial distribution of bonding electrons with possible light emission in the ultraviolet or visible regions. To obtain visible light from a gas laser, electronic transitions in the lasing medium will probably be required. It is necessary that the pumping reaction for the lasing substance specifically pump a limited number of electronic levels. Chemical pumping has great promise of such "specificity;" and, due to short lifetimes and low reagent mixing rate, pulsed devices will probably be more successful than CW devices in producing electronic transitions [Ref. 15].

C. METAL OXIDE REACTIONS

Prior to the operation of the first chemical laser Polanyi suggested that reactions of the type [Ref. 11]

$$M + XY \longrightarrow MX^* + Y \qquad (15)$$

where M is an alkali metal atom, XY is a covalent halogan or halide and MX is an ionic metal halide, show particular promise of producing chemical laser action. Recent results of work performed at the Los Alamos Scientific Laboratory by Walter W. Rice, Reed J. Jensen and others indicate the probable success of a metal atom oxidation laser in which the inversion results from an exothermic, atom-diatom exchange, chemical reaction of the simple metathesis thype.

The number of diatomic molecules MX* available as possible candidates can be reduced significantly as one considers the requirements for a visible gas-chemical hybrid laser system. To meet the exothermicity requirement the MX bond must be relatively strong; also, the MX molecules are required to have low lying electronic states and the system must be in the gas phase.

The metals of Group IIIA, B, Al, Ga, In, Tl, have low lying electronic states, form strong bonds and have high volatility. Of the metals of Group IVA, Sn, Pb and molecular radicals of the group hold promise. The compounds of the rare earths, particularly the halides and oxides, are extraordinarily stable and have a rich abundance of low lying electronic states. In conclusion, the oxides and halides of Groups IIA, IIIA, Sn, Pb and the rare earths are likely candidates. Examples of natural reagents, with weak bonds, to fuel these reactions are I_2, Cl_2, F_2, O_2, O_3 and NO_2.

W. W. Rice and R. J. Jensen [Ref. 13] report observation of intense laser pulses in an AlF system. The mechanism responsible for the lasing

was thought to be the exothermic chemical reaction

$$Al + F_2 \longrightarrow AlF^* + F$$
$$\Delta H = -122.5 \pm 2.1 \text{ kcal mole}^{-1} \qquad (16)$$

The radiation wavelength was in the range of 12.5μ to 13.5μ, well within the vibrational-rotational spectrum of the electronic ground state of the AlF molecule. The laser pulse was about 2μsec in duration and appeared to be quenched by heating of the lasing medium. The work by Rice and others at Los Alamos implies that when reaction (15) is exothermic, M may be almost any metal for XY = F_2, or XY may be almost any gaseous oxidizer for M = reactive metal. A complete summary of the work done on metal-oxidation lasers at Los Alamos Scientific Laboratory is given in Ref. 12.

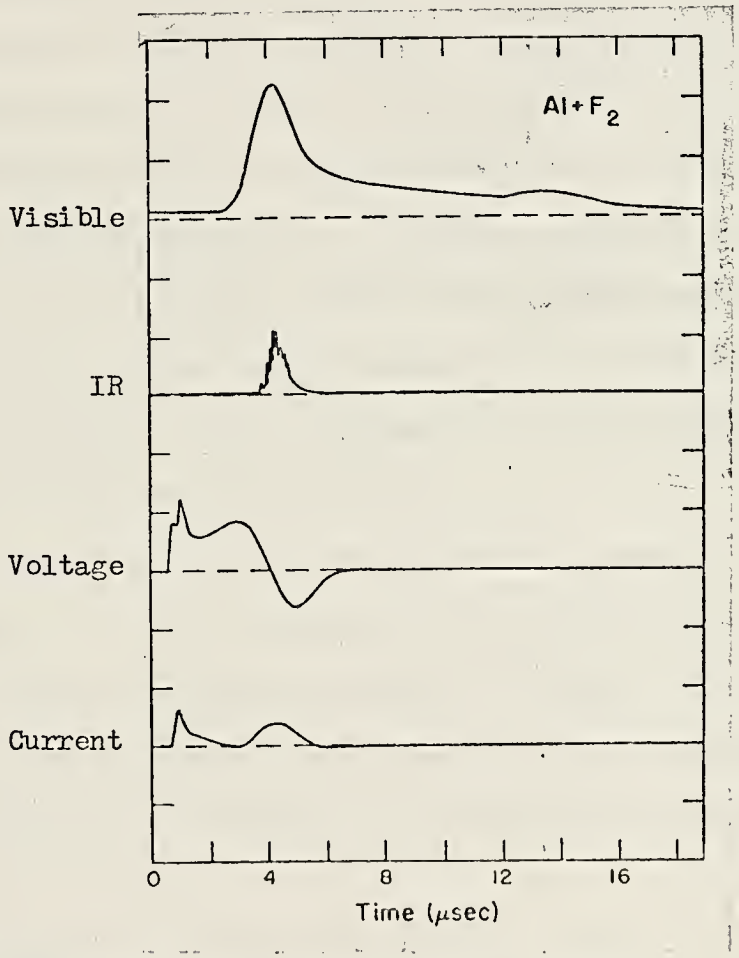

Figure 4. EXPLODING WIRE LASER OSCILLOGRAPHS SHOWING VISIBLE FLUORESCENCE, IR LASER PULSE, CAPACITOR VOLTAGE AND CURRENT FOR Al+F_2, EQ. (16), (Ref. 12).

D. METAL OXIDE LASER SYSTEM

1. General Description

The experimental setup of the metal oxide laser is shown in Figures 9 and 20. Appendic C consists of the design calculations for the laser tube and end pieces, the stability analysis of the optical cavity and calculation of the Gaussian spot size. Some of the system components have been borrowed from the previously described CH_3N_3 laser system, but the bulk of the system was constructed specifically for the metal oxide laser.

The entire gas system is constructed of stainless steel since pure oxygen is to be used in the experiments. All valves in the system are solenoid actuated and remotely operated from a portable control panel. The laser tube, optical cavity, detectors, all system piping and valves are located in a plexiglass enclosure to facilitate the use of a nitrogen atmosphere to conduct the experiments in. The laser system and optical components are mounted on a two-meter optical bench. Additional electronic equipment consisting of a dual trace oscilloscope, a memory scope, pressure monitoring equipment, and a pulse generator for the trigger circuit are located outside the plexiglass shield.

The high voltage capacitor bank is located in a wooden enclosure and the system plexiglass shield sits on top of the capacitor bank. The bank is discharged through a spark gap triggered by a 30 KV pulse. The entire electrical system is grounded to the negative side of the capacitor bank, which is grounded to the earth via an eight-foot copper rod sunk in the ground.

2. Optical System

The lasing medium is enclosed in a pyrex glass tube that is mounted in two stainless steel end pieces. The pyrex tube is 24 cm long with

a 22mm inside diameter. The tube is held in position by O-rings which are compressed against the tube with circular clamps. The O-rings also seal the vacuum at this point. The laser tube and end pieces are detailed in Figures 11 and 21.

The pyrex tube is capped by two identical end pieces made of monel and type 321 stainless steel. The end pieces can be completely disassembled and all metal-to-metal seals are made with viton O-rings. Brewster angle, NaCl windows are mounted with O-rings and stainless steel clamps to facilitate their replacement when needed. The fine wires used in the experiments are secured to the baffles by small copper clamps; to replace the wires after each experiment the end plate of each end piece must be removed. Each end piece also serves as a high voltage connector; the copper leads from the capacitor bank are bolted to the end pieces. Stainless steel fittings are mounted on each end piece to connect the laser tube to the gas handling system and to the vacuum system.

The laser tube was centered between two mirrors spaced 140cm apart. Gold-surfaced mirrors of 10-m radii of curvature and 1 inch in diameter were used in the optical cavity. One mirror had a 1-mm diameter hole through its center for output coupling. The optical cavity was aligned with a small He-Ne laser.

3. Vacuum System

The vacuum and gas handling system was designed to provide:

a. specific amounts of gas to the laser tube,

b. a means of exhausting pure oxygen and flushing of the laser tube,

c. a nitrogen atmosphere to conduct the experiments in,

d. remote control of the entire system during the experiments.

A schematic of the complete system is given in Figure 10. Plastic tubing is used between the laser tube and the vacuum system for electrical isolation; $\frac{1}{4}$-inch stainless steel tubing is used between all valves in the system and also to connect the gas cylinders to the system. Connecting the system to the oil diffusion pump, $\frac{1}{2}$-inch stainless steel tubing is used from the vacuum isolation valve (VP, Figure 10) to the manifold on the oil diffusion pump. The larger diameter tubing greatly reduces pumping time. Swagelok stainless steel fittings are used throughout the system. Ten Skinner solenoid-actuated valves with 3/16-inch diameter orifice and viton seal are used in the system. The valves are mounted on a stainless steel panel with all wiring connections and terminal boards on the back side of the panel away from the laser tube. A 15-foot cable connects the electrically operated valves with a portable control panel (Figure 22).

The laser tube, valves, piping, and all of the optical components are located inside a plexiglass enclosure which is purged and filled with nitrogen for the experiments. The enclosure is constructed of $\frac{1}{2}$-inch plexiglass, with the following inside dimensions: length, 84 inches; width, $16\frac{1}{2}$ inches; and height, 24 inches. The top is removable for major work on the system, and two removable front panels are provided to facilitate conducting the experiments. The nitrogen and oxygen are stored in metal cylinders outside the enclosure and connected to the system through Swagelok stainless steel bulkhead fittings. The gas flow rate is controlled by two-stage regulators. Provision is made in the system for future use of additional gases such as chlorine or florine.

An electrically driven mechanical forepump in line with a 4-inch oil diffusion pump can provide a vacuum of 10^{-6} torr. A large volume plenium is in the system to dilute any pure oxygen prior to pumping it

out of the system. An MKS Baratron type 170 series pressure meter using a capacitive-type detector head was used to monitor the system pressure and to measure the partial pressure of the gases used. The pressure range used was 0-100 torr. The diffusion pump also had a thermocouple detector to measure pressures less than 10^{-2} torr.

4. Electrical System

The electrical system consists of a portable remote control panel, Figure 22, and an isolation transformer for the electronic equipment used. A schematic of the electrical system is given in Figure 8. All of the system valves are remotely operated from this panel, which is connected to a socket mounted on the side of the plexiglass enclosure through a 15-foot cable.

A schematic of the vacuum and gas system is drawn on the front of the panel, with each valve represented by a red light with a toggle switch immediately below the light to operate that valve: valve open--light on; valve closed--light off. A test switch is provided that tests the lights through a relay. A main power switch and fuses are also provided on the panel.

5. High Voltage System

The high voltage system consists of the capacitor bank, the high voltage power supply, the high voltage charging control circuit and the firing circuit. A schematic of the system is given in Figure 12. The high voltage capacitor bank consists of two 7-μf, oil-filled, 25KV capacitors connected in series to give a total capacitance of 3.5μf. Copper bus bars, 3 by $\frac{1}{4}$ inch, are used to connect the capacitors. The entire system is grounded to the low side of the capacitor bank, which is grounded to the earth by an eight-foot copper rod sunk into the ground. The high voltage power supply is a New Jersey Electronics Model HA-51 variable

power supply, 0-30 KV at 0-10 ma. Charging current and voltage can be read from meters on the power supply front panel.

The high voltage charging circuit utilizes a portable control box, Figure 24, that provides four lights to indicate the condition of the capacitor bank. A schematic of the charging control circuit is given in Figure 13. The control box is connected to the charging control system with a ten foot cable; the components of the control system and the high voltage system are mounted on a panel inside the capacitor bank enclosure. A 0-20 μA ammeter calibrated as a 0-20 KV voltmeter is mounted on the outside of the capacitor bank enclosure and the main power switch for the charging control circuit is mounted next to the meter. All other switches and indicator lights are mounted on the control box. The output of the high voltage power supply is set on the front panel of the power supply with a Variac; an over-current limit switch is also set at the power supply. The desired voltage to which the capacitor bank is to be charged is set by a limit adjustment at the meter relay. The operation of the system (refer to Figures 12 and 13) is as follows:

Both power switches are closed, which lights the red power light on the control box and puts a dc voltage at terminals X and Y. Positioning the charge/discharge switch (S1) to the charge position de-energizes relay 4, which in turn de-energizes the Dump Relay and closes contacts which allow a small current to flow through relays 2 and 3. Depressing the charge button temporarily energizes relay 1 which closes the contacts that keep relay 1 energized and also the contacts which energize the Charge Relay, lighting a charging light. When the Charge Relay is energized, the contacts are closed and the capacitor bank begins to charge to the voltage set at the high voltage power supply. The charging path is from the power supply through the Charge Relay and R1, current limiting

resistor, to the high side of the capacitor bank. When the capacitor bank is charged to the voltage set at the meter relay, the meter switch closes, which shorts out R6 and greatly increases the current to relays 2 and 3; the increased current causes the relays to operate and lights the green ready light. Relay 3 closes contacts to keep the ready light lit, and relay 2 opens contacts to de-energize relay 1 and disconnect the meter-switch from the circuit. With relay 1 de-energized, the Charge Relay contacts open and the capacitor bank is charged and ready to fire. Once the bank has been fired, the charge/discharge switch is moved to the discharge position which energizes relay 4 and lights the amber dump light. Relay 4 also energizes the Dump Relay which discharges any residue voltage on the capacitor bank through the Dump Relay contacts and resistor R2 to ground. After firing, the charge/discharge switch has to be moved to the discharge position prior to charging the capacitor bank a second time.

The capacitor bank is connected to the laser tube with 3/8-inch copper tubing. The copper tubing is first covered with insulation and then covered with a copper shield that is grounded. The high side of the capacitor bank is connected directly to one of the stainless steel laser tube end pieces which serve as the high voltage terminals for the wire samples. The low (ground) side of the capacitor bank is connected to the other laser tube end piece through a spark gap which serves as a high voltage switch.

The spark gap, Figure 14, is made up of two $1\frac{1}{4}$-inch diameter polished copper hemispheres mounted on 5/8-inch diameter copper stems. The copper tubing from the capacitor bank is attached to the copper stems with set screws. The gap between the hemispheres is adjustable from zero to two inches. The firing trigger is applied through a tungsten electrode in series with a 100K Ω high voltage resistor. The spark gap is enclosed

by a $\frac{1}{2}$-inch plexiglass box; and the box is filled with argon to prevent deterioration of the copper hemispheres during operation.

The firing trigger is produced by an ILC PG-10 Pulse Generator. The output is a 0-500 volt pulse and a 20 volt sync trigger which can be produced at a rate of 40 pps. The trigger pulse is applied to the spark gap through an ILC Model T-105 pulse-forming network consisting of a 8μf, 500v oil-filled capacitor and a 60:1 step-up pulse transformer. The trigger circuit is shown as part of the high voltage system in Figure 12.

6. Instrumentation

The instrumentation setup was arranged to monitor IR radiation from the laser cavity, visible radiation from the side of the laser tube and capacitor voltage during an experiment. In addition the exploding-wire circuit current, using a 5000:1 current transformer, was monitored to analyze the electrical characteristics of the circuit; the laser heads were shorted with a copper cable during the current measurements.

The infrared detector used was a gold-doped germanium photoconductive infrared detector with an active area of $5mm^2$. The detector element is mounted on a gold-plated-copper heat sink enclosed in a SBRC Model No. 40742 metal dewar with an Irtran 2 window. The dewar must be pumped to 10^{-4} torr for a minimum time of 1 hour and is cooled to $77^{\circ}K$ with liquid nitrogen. The detector has a range from 1.0 microns to 11.0 microns with a peak at 5.0 microns and a smaller peak at 10.6 microns. The detector is biased for a 1 volt output per watt of input with response less than 100 nanosec. The bias circuit and detector connections are shown in Figure 7. An anti-reflection coated germanium lens with a focal length of 25mm is mounted on the dewar between the detector and the optical cavity. The lens reduces the visible radiation input to the detector. The

infrared detector output is monitored with a Tektronic Type 549 Storage Oscilloscope and Type 1A6 differential amplifier plug-in unit.

Visible flourescence is monitored from the side of the pyrex laser tube using a photo multiplier. The output of the photo multiplier is fed directly to a Type 53/54D high gain differential amplifier plug-in unit in a Tektronic Type 551 Dual Beam Oscilloscope. A capacitive network and copper shielding on the coax connection cable is necessary to reduce interference from the spark gap trigger signal.

The capacitor voltage during discharge is monitored using a Tektronic P6015 high voltage probe connected to the high side of the capacitor. The probe provides 1000:1 attenuation of the signal before it is applied to the input of a Type 53/54D high gain differential amplifier in a Type 551 dual beam oscilloscope.

Both oscilloscopes are triggered externally by a 20-volt sync signal from the PG-10 pulse generator. A variable 0-70 μsec delay line in the spark gap trigger circuit allows the scopes to be triggered 10 μsec prior to the spark gap being triggered. Both oscilloscopes are mounted with Tektronic Series 125-1.9-1:0.85 magnification Polaroid cameras. Polaroid type 107, 3000 speed film was used.

E. METAL OXIDE EXPERIMENTAL TECHNIQUE

1. Exploding Wires

In order to produce the required population inversion, and to exceed optical losses and the non-ideal conditions often encountered in the laboratory, a laser device should produce at least 10 μw of power. If a quantum efficiency of one 10-μm IR photon per metal atom and a reaction rate of 10^{13} cm^3/mole-sec are assumed, the metal atoms would have to be present in a concentration of 5.5×10^{12} cm^{-3} to produce the needed power

from a 10-cm^3 volume (volume of laser tube used in this experiment was 108 cm^3). Electrical explosion of metal wires and foils is known to produce many orders of magnitude higher density than the required 10^{12} cm^{-3} [Ref. 12].

The exploding wire phenomenon exhibits a varied behavior pattern which is dependent upon the type of experiment performed. According to one theory, the process takes place in two separate phases, the first known as the burst phase and the second as the restrike phase, with a current minimum (dark pause) between the two phases. During the dark pause, the wire is reduced to a high-density colloid of liquid-metal droplets in a matrix of metal vapor. Since no continuous conduction path exists and the vapor density provides an electron mean free path less than that required to accelerate the thermionic electrons to avalanching velocities, a high resistance exists and the voltage climbs to a maximum. Expansion of the vapor results in lower densities and allows avalanching and restrike to occur. Reference 2 discusses the physics, chemistry and spectroscopy of electrically exploded wires.

2. Operation of Gas and Vacuum System

The valves are electrically operated from a remote control panel, Figure 22, and system pressures are read from the MKS digital readout, Figure 23. (Refer to Figure 10 for valve location and functions within the system.)

The system is first pumped down using the forepump with valves VP, P, V and MKS open. When the system pressure has reached minimum, 0.00 on readout, valves VP and P are closed. Valve 0 is momentarily opened to pressurize system with O_2 to 80-90 torr; the gas flow rate is controlled by regulators located on the gas storage bottles. Valve P is opened to bleed O_2 from laser tube to plenum; this will reduce pressure

to about 8 torr. Then close valves V and P. Valve O is then momentarily opened to increase O_2 to desired pressure for laser shot.

After the laser shot, the gaseous products in the laser tube are exhausted through valve EXH. Valve DET and P are opened to dilute the O_2 in the plenum and then the plenum is pumped down with the forepump through vlaves VP and P.

3. Materials

The manufacturers and purities of the gases and metal wires used in these exploding wire experiments are as follows: Air Reduction Company, Inc., Grade 4 (ultra-pure) O_2; Materials Research Corp., marz grade, .005" Al wire, 99.999%, marz grade, .020" indium wire, 99.99+%; Consolidated Companies, .005" copper wire, purity unknown.

4. Metal Oxide Experimental Procedure

Prior to each laser shot (experiment) it is necessary to clean the laser tube and heads and install a test wire in the laser tube. The laser heads are both disassembled, see Figure 11 for laser head detail, and the spacers and explosion baffles removed. After cleaning and installing a new pyrex laser tube, if needed, a test wire is mounted in a wire clamp on one baffle. The baffle is placed in the laser head and the wire threaded through the laser tube. The remaining baffle with clamps on it is inserted in the opposite laser head and the test wire is mounted. The laser heads are now reassembled. The optical cavity is aligned, see Appendix B, prior to beginning experiments; and the alignment is checked prior to each shot.

After mounting the wires, the plexiglass covers are replaced and the box is filled with N_2 through valve NE. The laser tube is charged with O_2, Section III.E.2, and the instrumentation is set up as described in Section III.D.6. The capacitor bank is charged to the desired voltage

(15KV for most of the shots; operation of charging system described in Section III.D.5). The laser shot is then initiated by depressing the manual trigger switch on the face of the PG-10 pulse generator.

F. RESULTS AND DISCUSSION

1. Exploding Wire

The electrical behavior of the exploding wire circuit was looked at briefly. Current and voltage characteristics were obtained by placing a copper shorting strap between the laser heads. Both the current transformer and the high voltage probe yielded underdamped sine waves with a peak current of 2.5KA and a ringing period of 14μsec (frequency of 77KHz).

During the exploding wire experiments, vaporization of the test wire occurs. The burst patterns deposited on the laser tube walls indicate both wire segmentation and vapor dispersion during the expanding phase of the event. The striation patterns obtained during these experiments are typical of results obtained by other experiments and are shown in Figure 15.

2. Metal Oxides

Experiments with three different metals were performed in an attempt to produce lasing by chemical pumping. The exploding wire phenomenon was used to produce metal atoms in a vapor. The experiments were necessarily pulsed due to the nature of exploding wires.

Lasing with AlO was attempted first. The reaction

$$Al + O_2 \longrightarrow AlO + O$$
$$\Delta H = 10.74 \text{ kcal mole}^{-1} \qquad (17)$$

is mildly endothermic and was not expected to yield positive results. The possibility of molecular excitation from the electrical energy deposited during the exploding wire event existed, but did not materialize.

Experiments performed by Rice and others at Los Alamos on "Shocked Plate Vaporization Lasers" give fairly conclusive evidence that no excitation is due to the exploding wire event [Ref. 12].

An oscillograph of the output of the IR detector, Figure 16, does not indicate any IR emission during the shot. Several shots were done at 15KV and about 20 torr O_2 with Al wires. There was no detectable IR emission from any of the shots. Pressure reduction averaged 1.30 torr during the reactions with O_2 at about 20 torr and 3.45 torr when the reaction was initiated at about 46 torr O_2. The pressure reduction can be interpreted that the reaction given by equation (17) took place. Output signals from the photomultiplier and the high voltage probe were unusable due to interference from the trigger signal.

One laser shot was performed using Cu wire in an O_2 atmosphere. No IR emission was detected, Figure 17, and no voltage or photomultiplier traces were recorded. The shot was performed at 15KV; a pressure drop from 21.05 to 20.31 torr O_2 indicates that the following reaction probably occurred:

$$Cu + O_2 \longrightarrow CuO + O \qquad \Delta H = -37.74 \text{ kcal mole}^{-1} \qquad (18)$$

This reaction is medium exothermic and the energy available is within the vibrational-rotational levels in the ground state of CuO.

The third attempt was using In wire in O_2. InO was the most fruitful of the three species investigated. An IR pulse was observed during the first μsec of the reaction, Figures 18 and 19, the burst phase of the exploding wire. The shot was performed at 15KV and 22.9 torr O_2. A pressure reduction of 2.1 torr during the reaction indicates that the following reaction probably took place:

$$In + O_2 \longrightarrow InO + O \qquad \Delta H = -68.38 \text{ kcal mole}^{-1} \qquad (19)$$

The reaction is medium to high exothermic and the energy available is well within the range necessary to excite rotational-vibrational transitions of the InO molecule. Several shots were performed with In wire at varying pressures of O_2. Due to an increasingly severe interference problem between the detectors and the spark gap trigger pulse the results of the subsequent experiments were not useful. Due to the greater mass of the .020" In wire over that of the smaller Al and Cu wires, vaporization in the In shots was incomplete using 15KV with the 1.5μf capacitor; this can be seen by examining the pyrex laser tubes in Figure 15.

Several attempts were made to explode Al wires in a vacuum prior to exploding them in O_2. A well-known but interesting phenomenon was encountered. When the Al wire was mounted in a vacuum, Al atoms would evaporate from the wire creating a very low density Al vapor in the laser tube. When capacitor bank voltage was increased to 3-5KV, the Al vapor would ionize, indicated by a slight pressure rise, and discharge the capacitor bank to ground through the ionized vapor columns that were within the plastic tubing that insulated the laser heads from the rest of the system. When the laser tube contained the Al vapor (pressure less than 10^{-2} torr) without the laser heads electrically connected, bursts of blue-green light would travel down the laser tube at about 20 cm/sec. The system pressure would increase slightly with each burst, indicating that the Al vapor was being ionized. The blue-green emission is characteristic of the Al atom. The same results were observed with In wires in a vacuum, and no attempt was made to explode Cu wires in a vacuum.

G. CONCLUSIONS AND RECOMMENDATIONS

A metal oxide laser system was designed and constructed. The preliminary experiments performed did not succeed in producing lasing action in

the diatomic molecules tested. The results of the In wire shots looked promising and lasing may be obtained with more work. The low peak current of 2.5KA in the shorted exploding wire circuit indicate that the dc resistance of the circuit is a little high. The major problem encountered was the severe rf interference in the detectors and scopes from the spark gap trigger. That interference source has been isolated to the pulse transformer.

The results of these experiments show that a useful research tool has been constructed. Recommendations for future experiments are:

(1) Redesign trigger circuit to eliminate the rf interference,

(2) Reduce the exploding wire circuit dc resistance by changing the position of the test wire clamps to the laser head body from the explosion baffles (see Figure 9),

(3) Conduct further experiments with In wire at various O_2 pressures,

(4) Conduct further experiments with O_2 using Tl, Ti and the rare earths,

(5) Explore the potentials of other oxidizers such as O_3 and Cl_2.

APPENDIX A. CH_3N_3 OPTICAL ALIGNMENT PROCEDURE

The optical system is aligned such that the horizontal axis of the optical cavity coincides with the horizontal axis of the laser tube. A low power laser is used to align the system. The procedure is as follows (see Figure 5):

1. Remove the detector and M_1; adjust M_3, the pinhole and the position of the alignment laser until the laser beam coincides with the optical axis of the laser tube.

2. Place the gimbal mount with M_2 in position such that the laser beam falls exactly onto the center of M_2.

3. Align M_2 by adjusting the gimbal controls until the reflected beam coincides exactly with the original beam. This can be achieved by adjusting the gimbal controls until the reflected beam falls onto the pinhole.

4. Replace M_1 in its gimbal mount in position so that the alignment beam falls onto the hole in the center of the minor and is reflected by M_2.

5. Adjust the gimbal controls of M_1 until the beam reflected from M_1 coincides with the beam reflected from M_2.

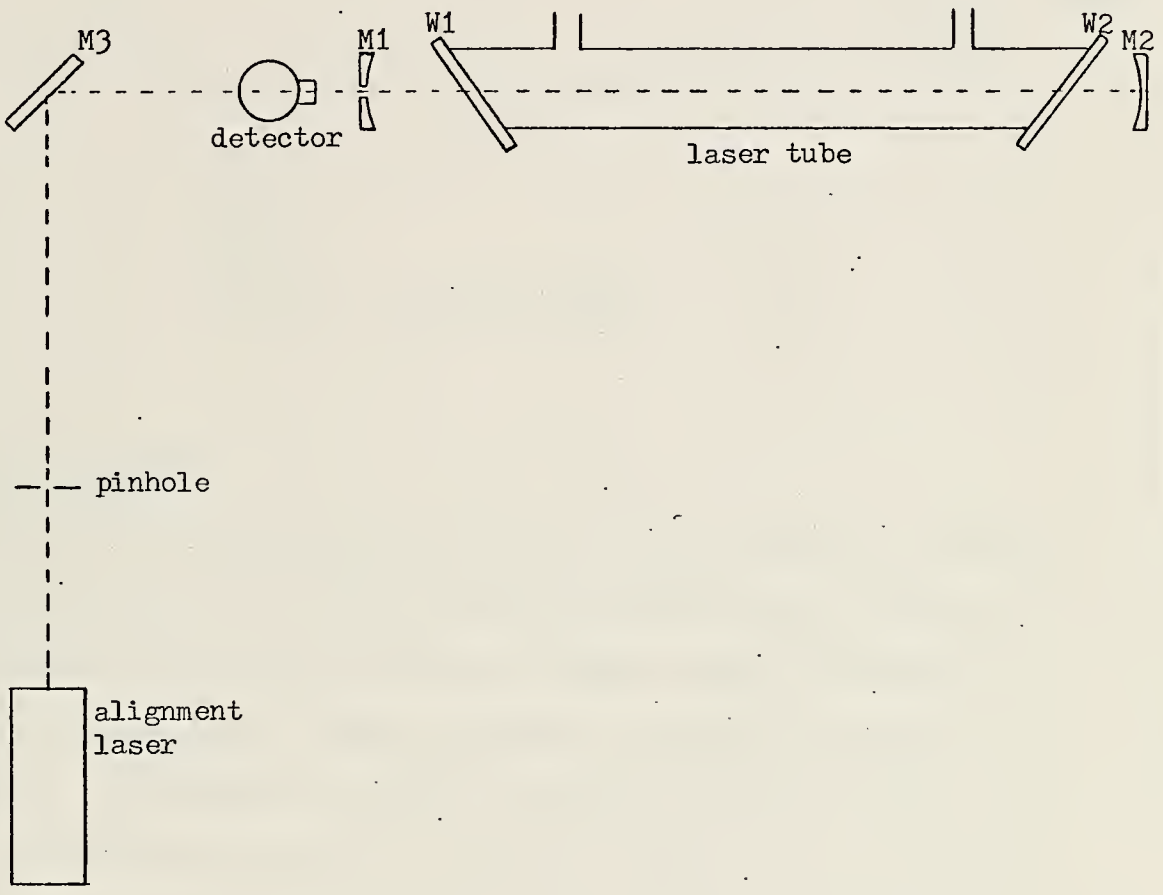

Figure 5. CH_3N_3 LASER OPTICAL SYSTEM

APPENDIX B. METAL OXIDE OPTICAL ALIGNMENT PROCEDURE

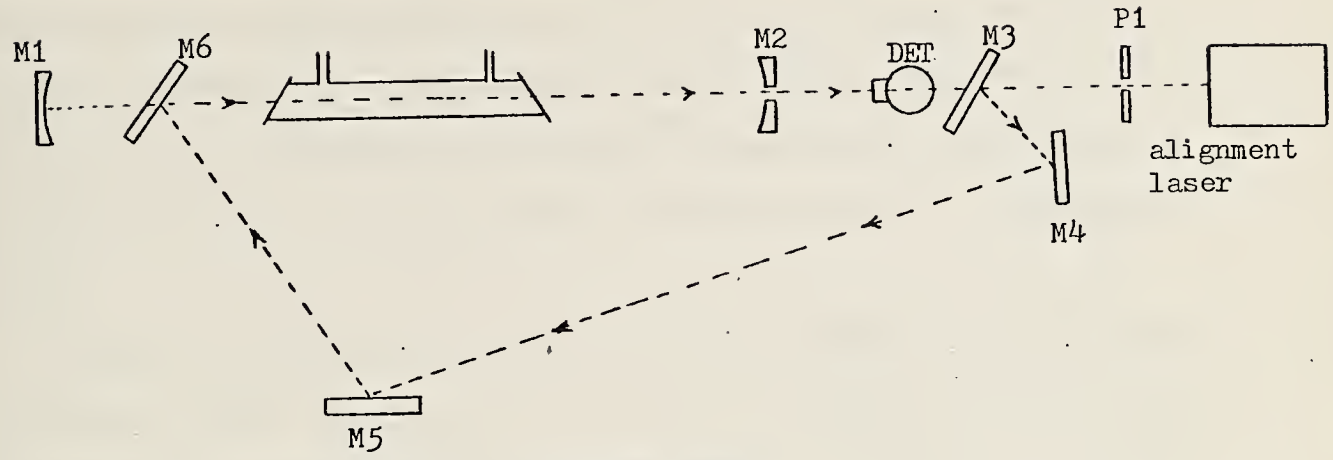

Figure 6. ALIGNMENT SETUP

Alignment Procedure

The optical cavity, detector and laser tube are mounted on a heavy, 2-meter optical bench to ensure mechanical stability and to allow the NaCl windows and pyrex laser tube to be changed without disturbing the alignment of the cavity. Refer to Figure 6 to follow the steps of the alignment. A He-Ne laser (λ=.6328 m) was used to align the system. End mirrors M1 and M2 are mounted in 3-degree-of freedom mounts; the height and horizontal position of the mirrors may be adjusted and the angle about both the vertical and horizontal axis may be adjusted.

Mirrors M2, M3, M6 and the detector are removed from the optical bench. Then the alignment laser, pinhole, P1, and end mirror M1 are arranged as shown in Figure 6. Adjust the laser beam height so that the beam ray goes through the pinhole, is exactly centered on the NaCl laser windows and coinsides with the horizontal axis of the laser tube; adjust horizontal and vertical position of M1 so that the laser beam is in the exact center

of the mirror. Rotate M1 about the horizontal and vertical axis until the laser beam is reflected back through the laser tube and impinges on P1 at the center of the pinhole. Replace mirror M2 in such a position to make the optical cavity 141cm long. Adjust the vertical and horizontal position of M2 such that the alignment beam impinges on the hole in the mirror and is reflected by M1. Now adjust the vertical and horizontal angle of M2 until the reflected beam is exactly aligned with the center of M1.

Replace the detector in the system with the window facing the alignment laser; adjust the position of the detector platform for proper height such that the alignment beam falls on the center of the detector window. Replace mirrors M3 and M6 and adjust the positions of M3, M4, M5 and M6 to reflect the alignment beam down the center of the laser tube to hit mirror M2 exactly in the center so that a portion of the beam passes through the hole in M2. Face the detector window towards mirror M2 and position it such that the beam falls directly onto the center of the window and detector element. Mark the position of the detector in order that it may be removed without realigning the system. Remove the alignment mirror, M6, for operation of the system.

APPENDIX C. OPTICAL RESONATOR CALCULATIONS

The optical cavity is an optical resonator, Figure 6, with the distance between the mirrors, L, equal to 140cm and the mirror radii, R_1 and R_2 equal to 10m. The inside diameter of the laser tube, D, is 22mm; the inside diameter of the NaCl window aperature, r, is 10mm and the distance from the centers of the laser tube to the NaCl windows, z, is 23.8cm. The center of the laser tube is also the point of minimum spot size. All calculations made assume a wave length, λ, of 10.6μm.

An optical resonator is stable, if [Ref. 17]:

$$0 \leq g_1 g_2 \leq 1 \tag{C-1}$$

where

$$g_1 = 1 - \frac{L}{R_1} \qquad g_2 = 1 - \frac{L}{R_2} \tag{C-2}$$

Using the valves for L, R_1, and R_2 we get $g_1=g_2=.86$ which gives

$$0 \leq (.86)^2 \leq 1$$

Therefore this configuration is optically stable.

The laser beam spot size at any distance from the center of the cavity is given by [Ref. 17]

$$W = \left[\frac{\lambda}{2\pi} \cdot \frac{b^2 + 4z^2}{b} \right]^{1/2} \tag{C-3}$$

where

$$b = \sqrt{4S(R_1 - S)} \tag{C-4}$$

and

$$S = d(R_2 - d)/(R_1 + R_2 - 2d), \quad d = 2z \tag{C-5}$$

Then, at the NaCl windows, (z=23.8cm) the spot size is W=2.947mm.

The minimum spot size at the center of the cavity, z=0, is given by

$$W_o = \sqrt{b\lambda/2\pi} \qquad \text{(C-6)}$$

which gives W=2.93mm.

The radius of the window aperture required for maximum transmission is given by

$$r = \frac{3}{2} W = 4.420\,\text{mm} \qquad \text{(C-7)}$$

The design window aperture is r=5mm which should give satisfactory performance.

The spot size at the mirrors is given by

$$W = \sqrt{\frac{\lambda}{\pi}} \left(\frac{R_1}{R_2} \cdot \frac{R_2 - L}{R_1 - L} \cdot \frac{R_1 R_2 L}{R_1 + R_2 - L} \right)^{1/4} \qquad \text{(C-8)}$$

which gives W=3.04mm.

APPENDIX D. DRAWINGS

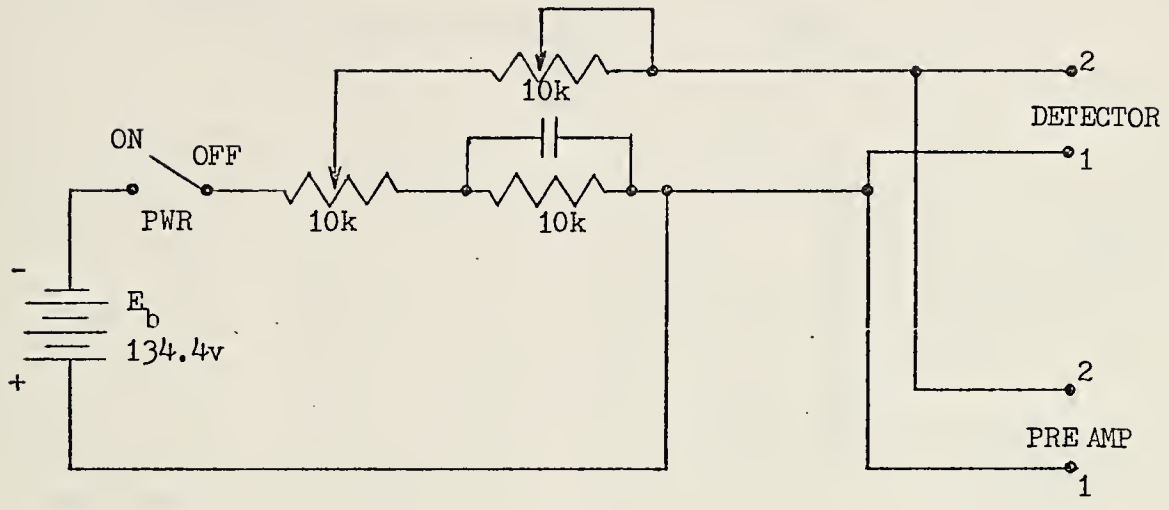

Figure 7. DETECTOR BIAS CIRCUIT

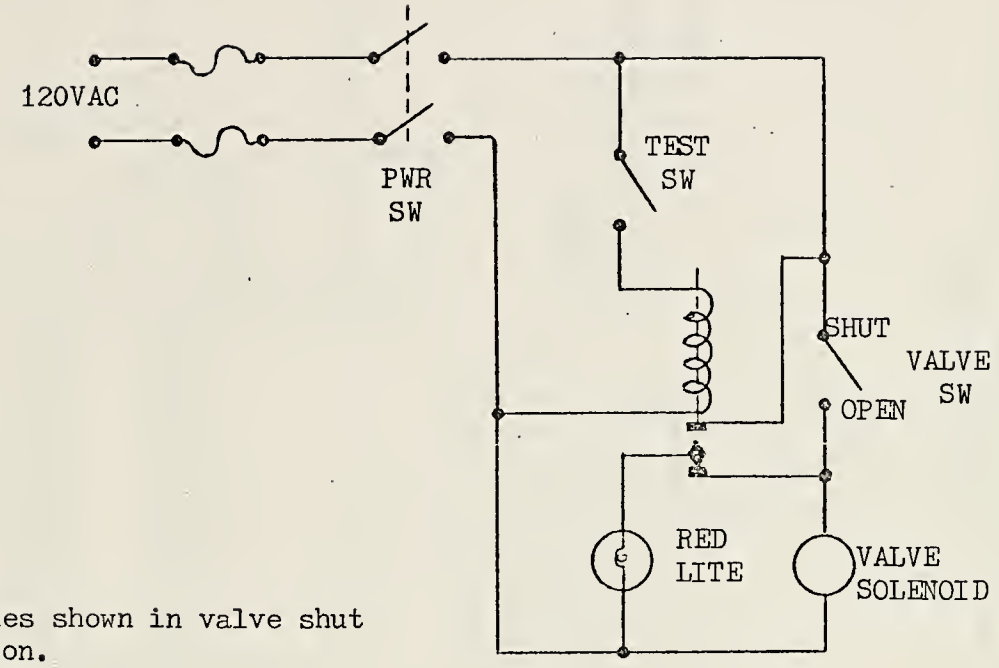

Switches shown in valve shut position.

Figure 8. TYPICAL VALVE CONTROL CIRCUIT

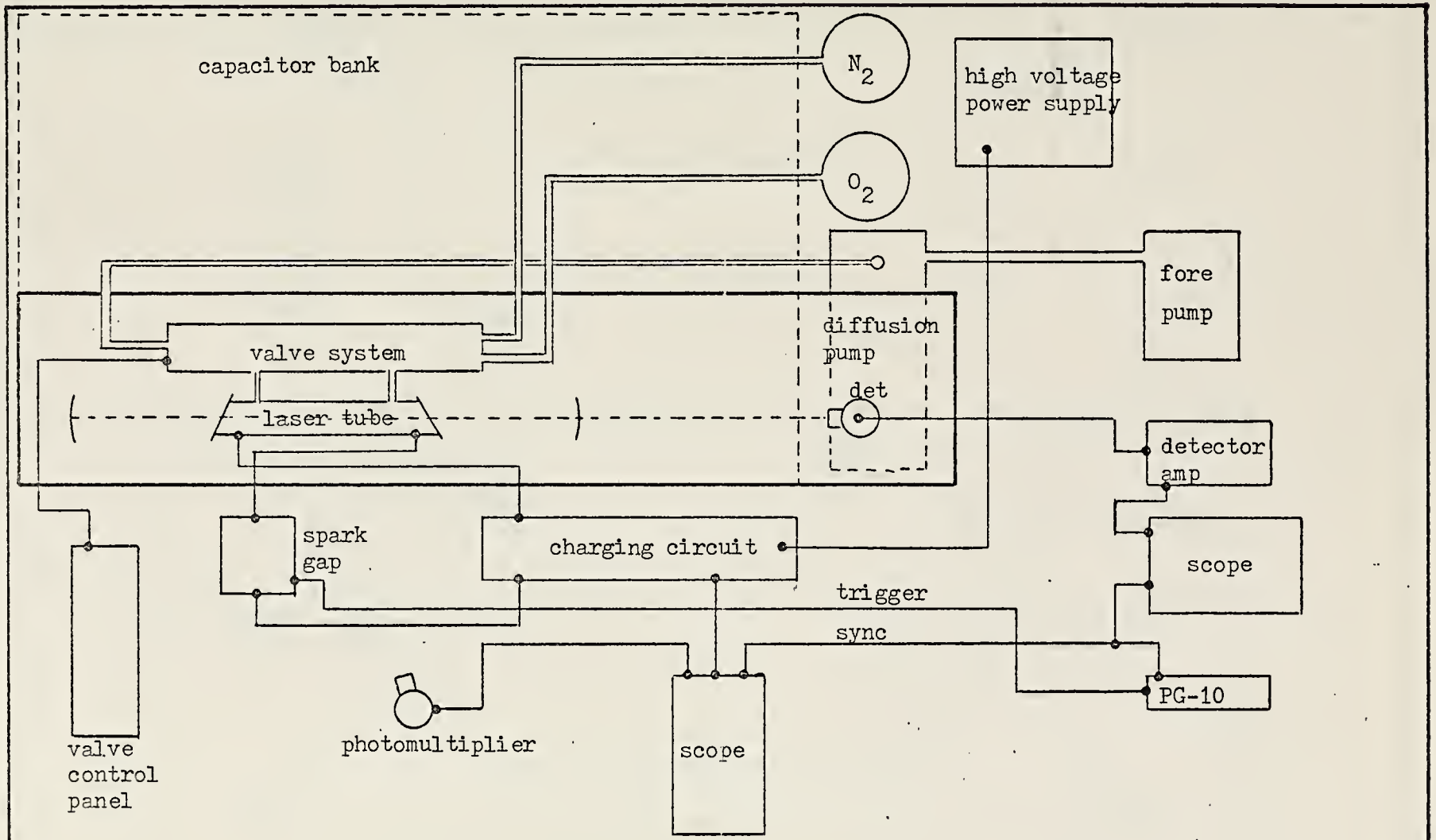

Figure 9. EXPERIMENTAL SETUP

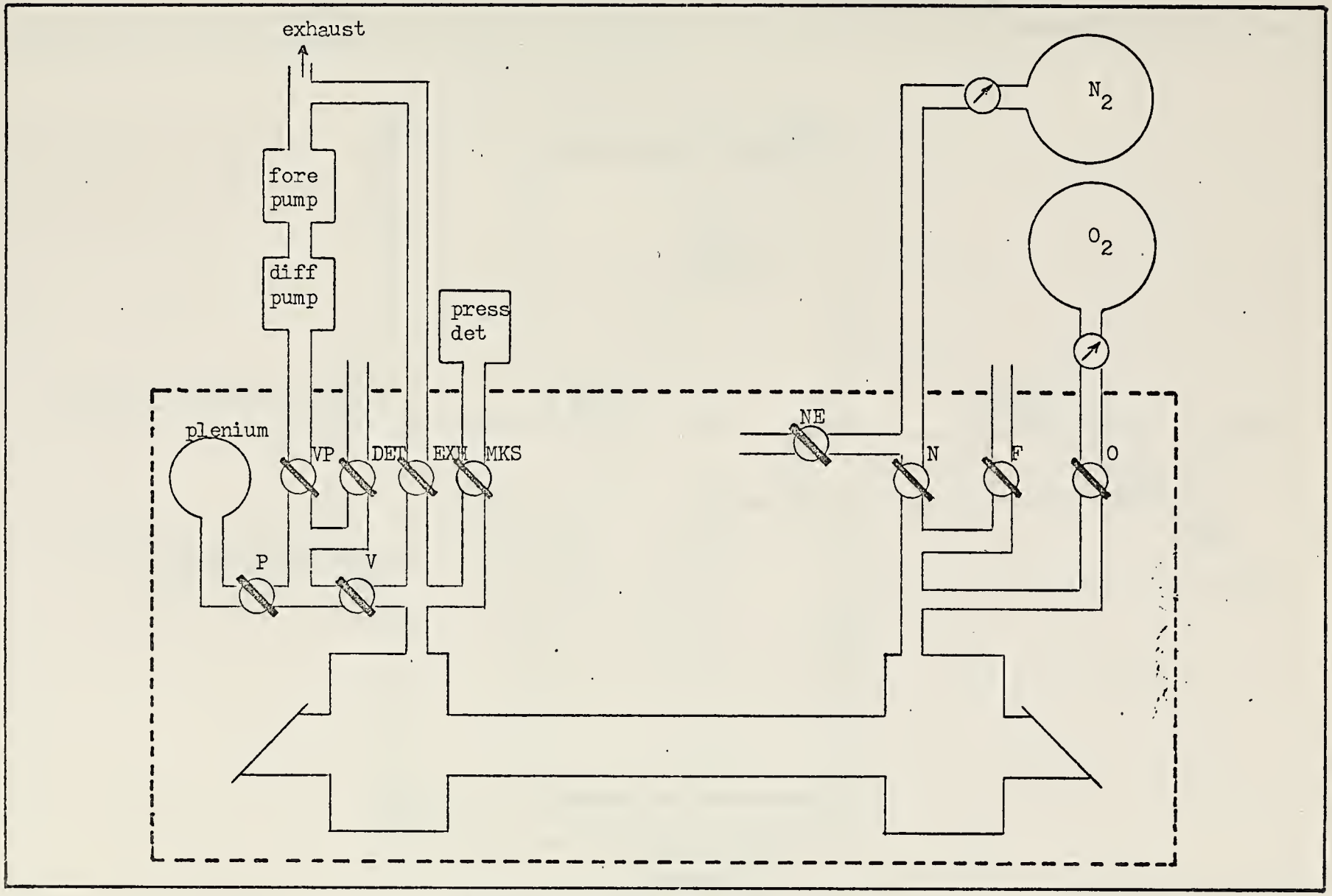

Figure 10. VACUUM AND GAS SYSTEM

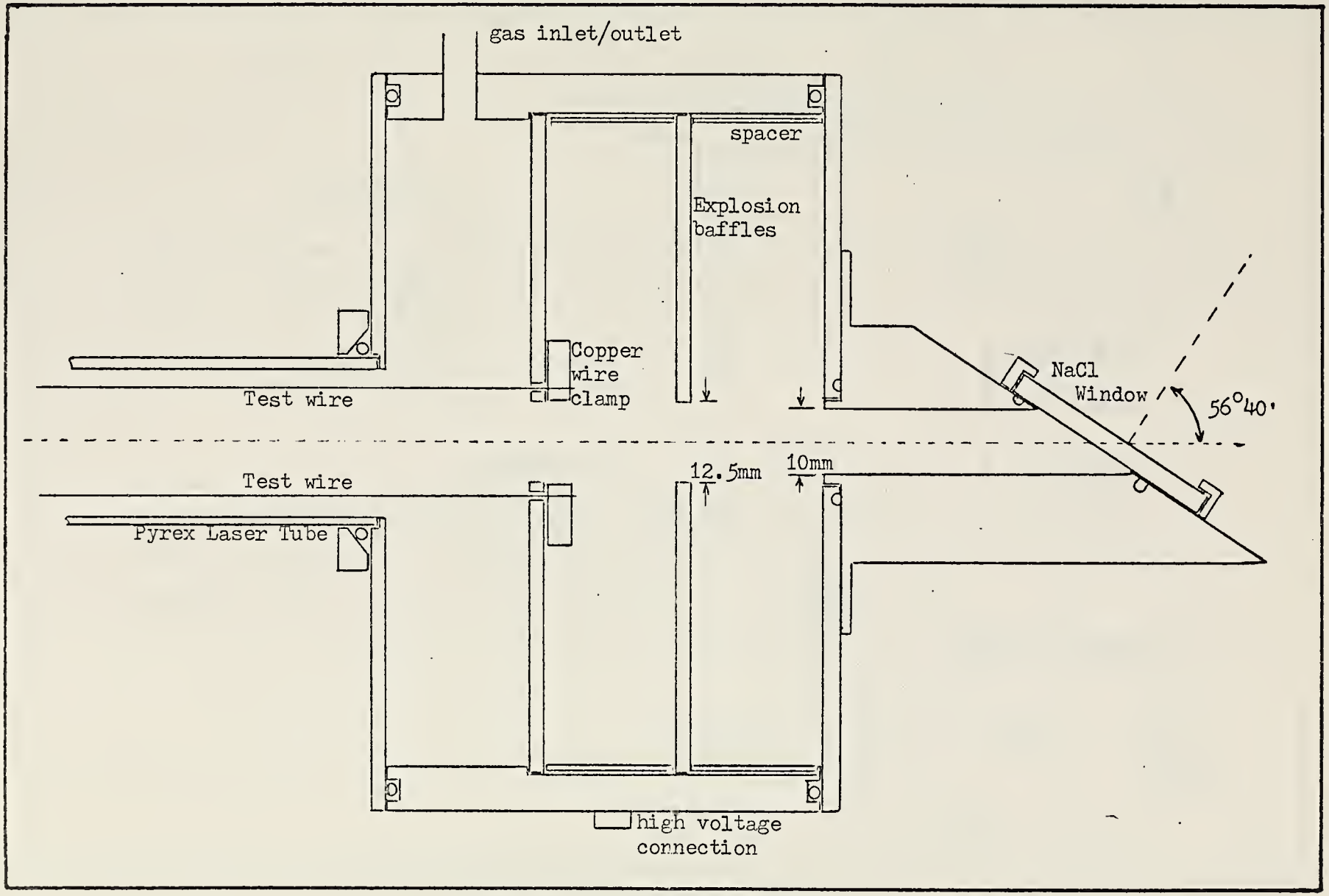

Figure 11. LASER HEAD DETAIL

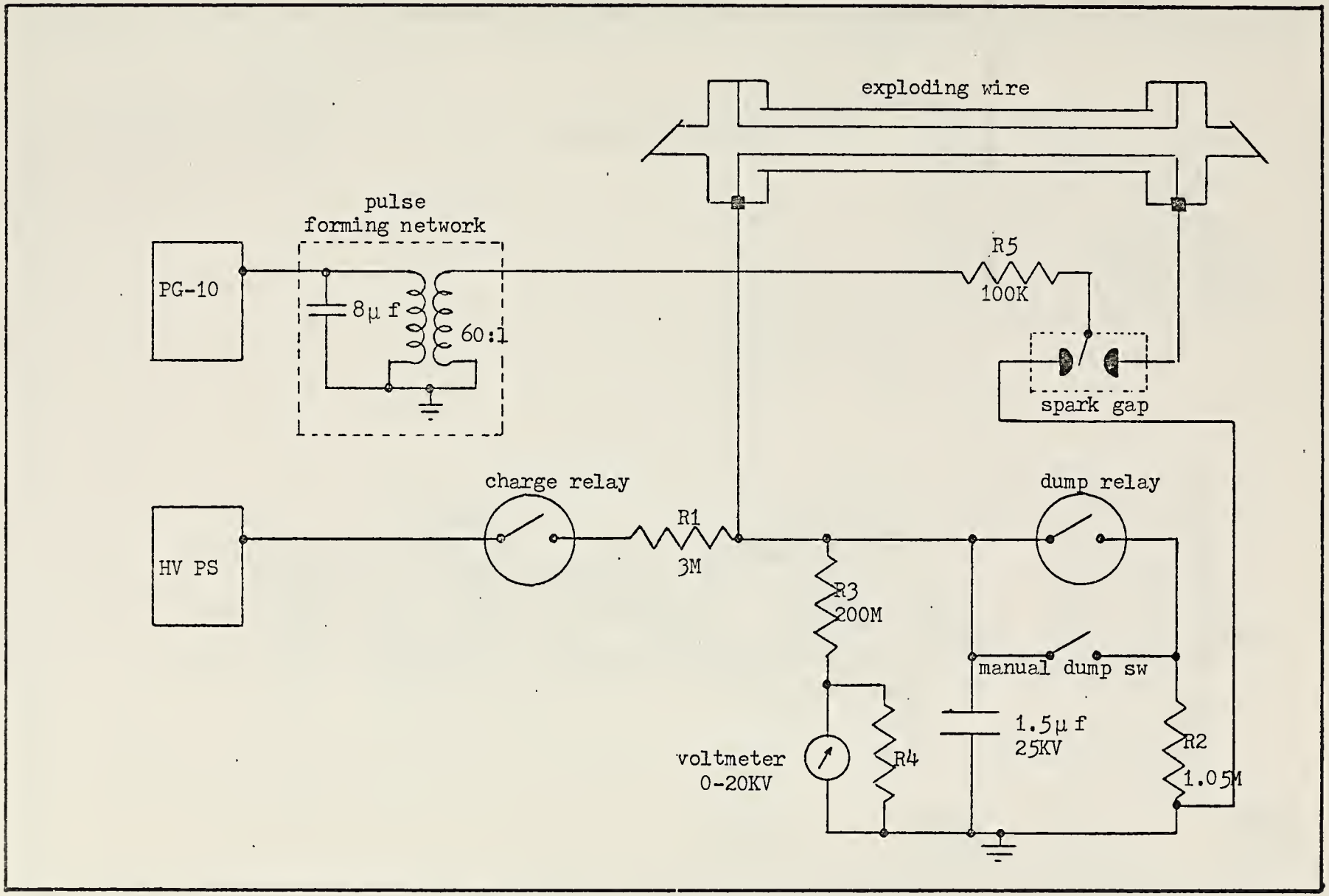

Figure 12. HIGH VOLTAGE SYSTEM

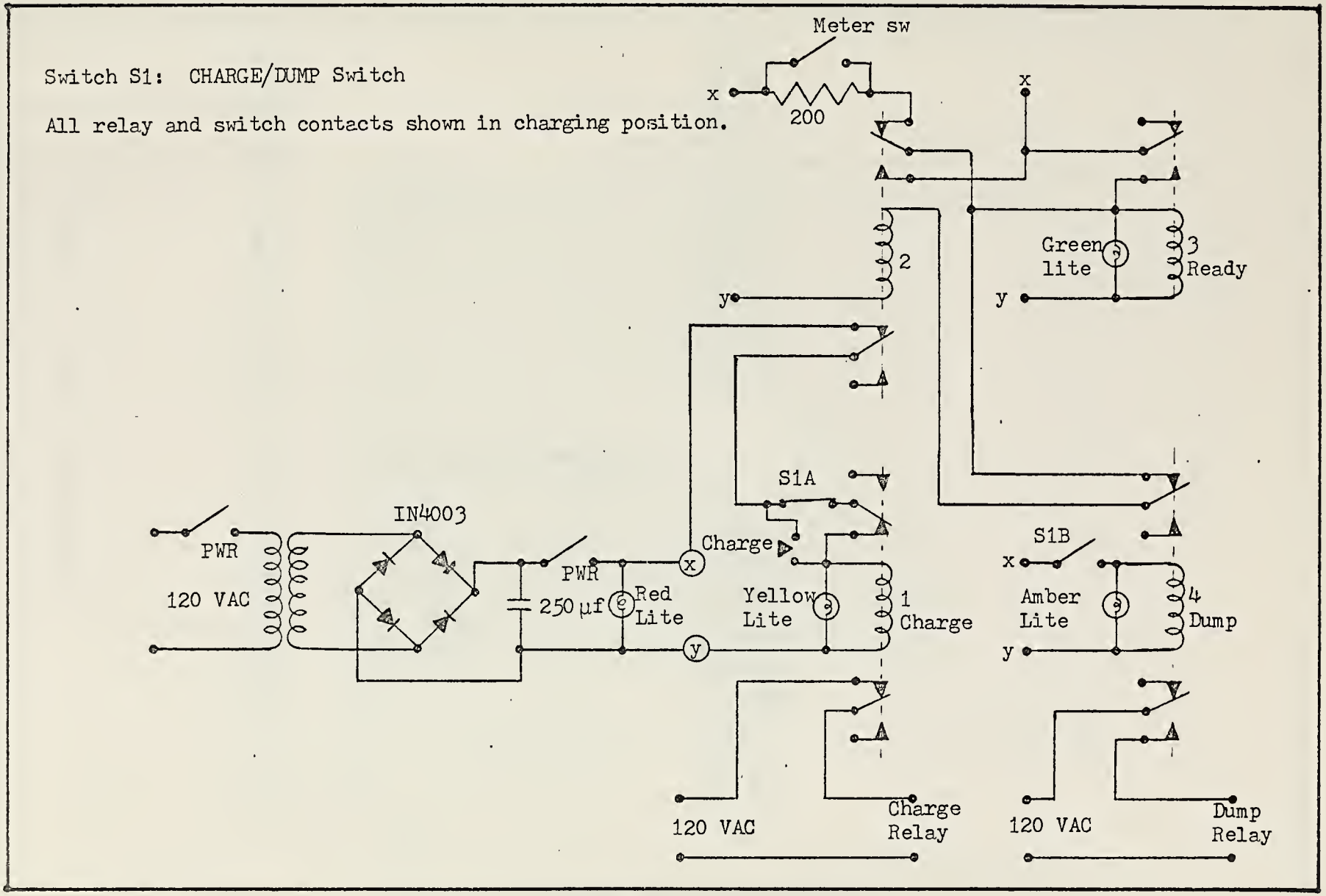

Figure 13. CHARGING CONTROL CIRCUIT

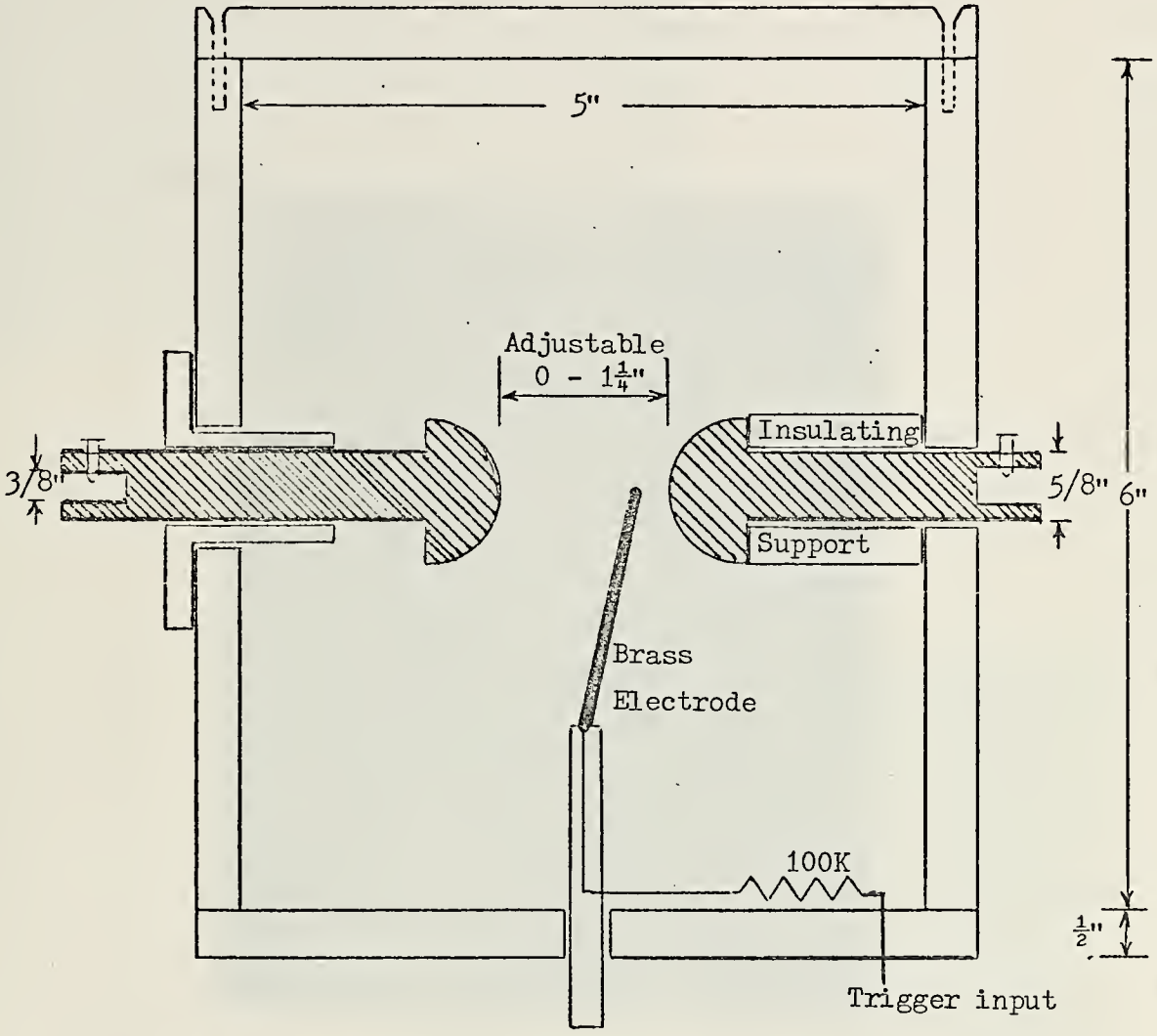

Spark Gap Electrodes are 1¼". Copper hemispheres mounted on 5/8" copper rods. Enclosure and supports are ½" plexiglass.

Figure 14. SPARK GAP CONSTRUCTION

APPENDIX E. PHOTOGRAPHS

Figure 15. EXPLODING WIRE STRIATION PATTERNS. Left to right: aluminum, copper and indium.

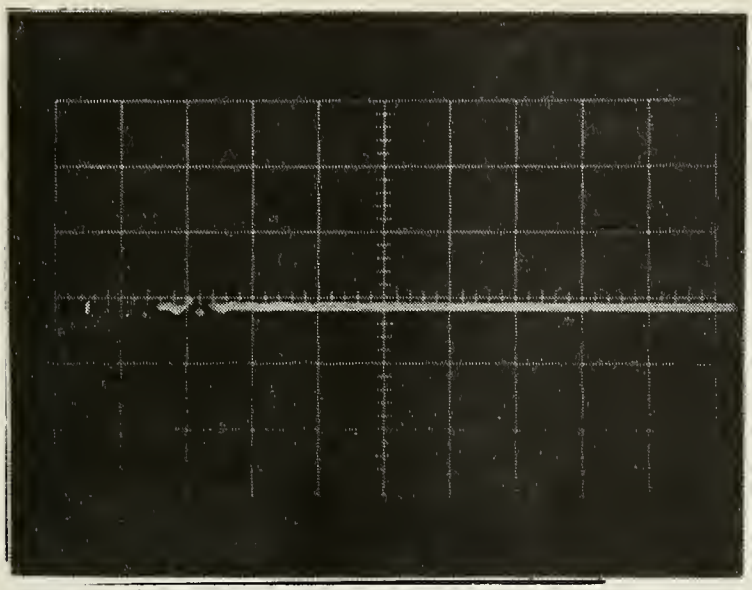

Figure 16. IR DETECTOR OUTPUT, AlO.
vertical: 500 mv/cm
horizontal: 1 μsec/cm

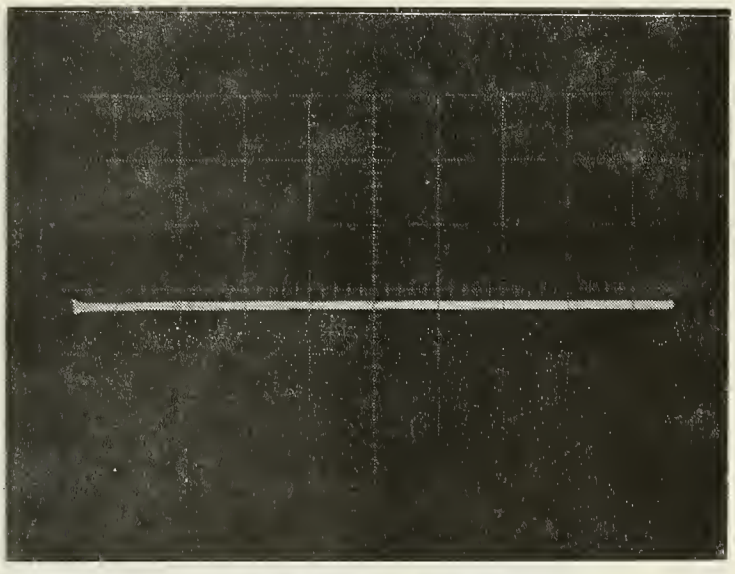

Figure 17. IR DETECTOR OUTPUT, CuO.
vertical: 200 mv/cm
horizontal: 5 μsec/cm

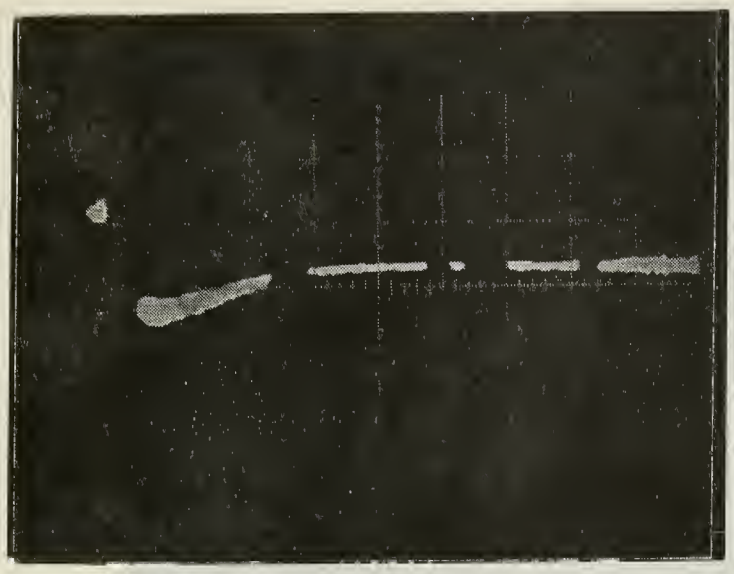

Figure 18. IR DETECTOR OUTPUT, InO.
vertical: 100 mv/cm
horizontal: 0.5 sec/cm

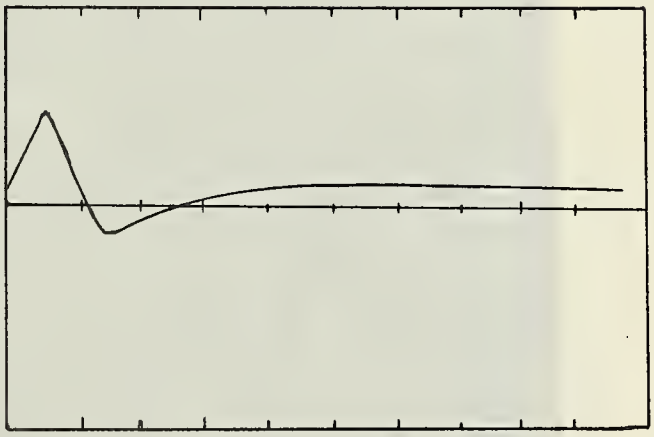

Figure 19. TRACE OF IR DETECTOR OUTPUT FOR InO.

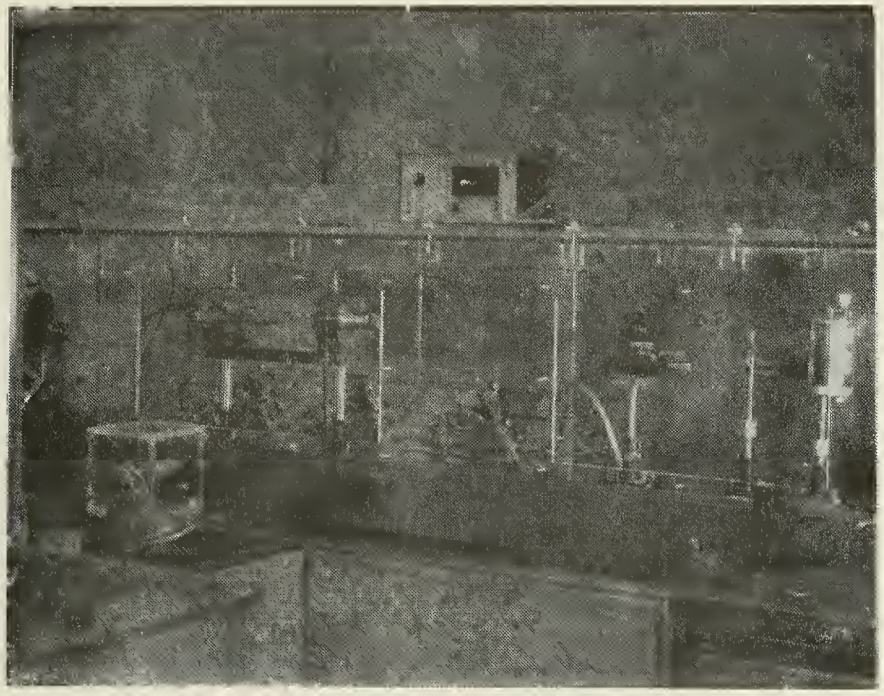

Figure 20. EXPERIMENTAL SETUP

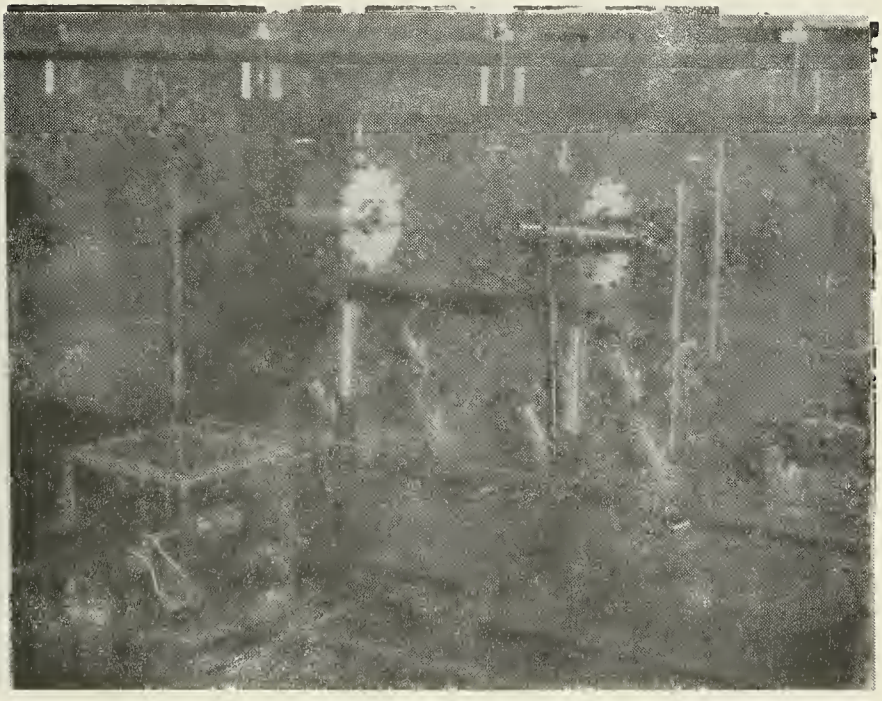

Figure 21. LASER TUBE AND LASER HEADS

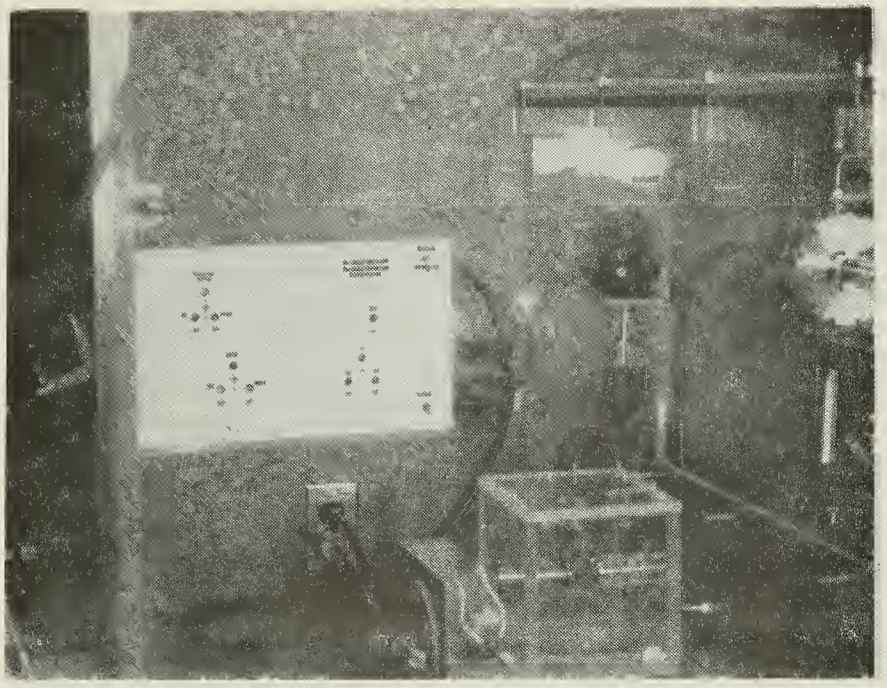

Figure 22. VALVE CONTROL PANEL AND SPARK GAP

Figure 23. LASER INSTRUMENTATION

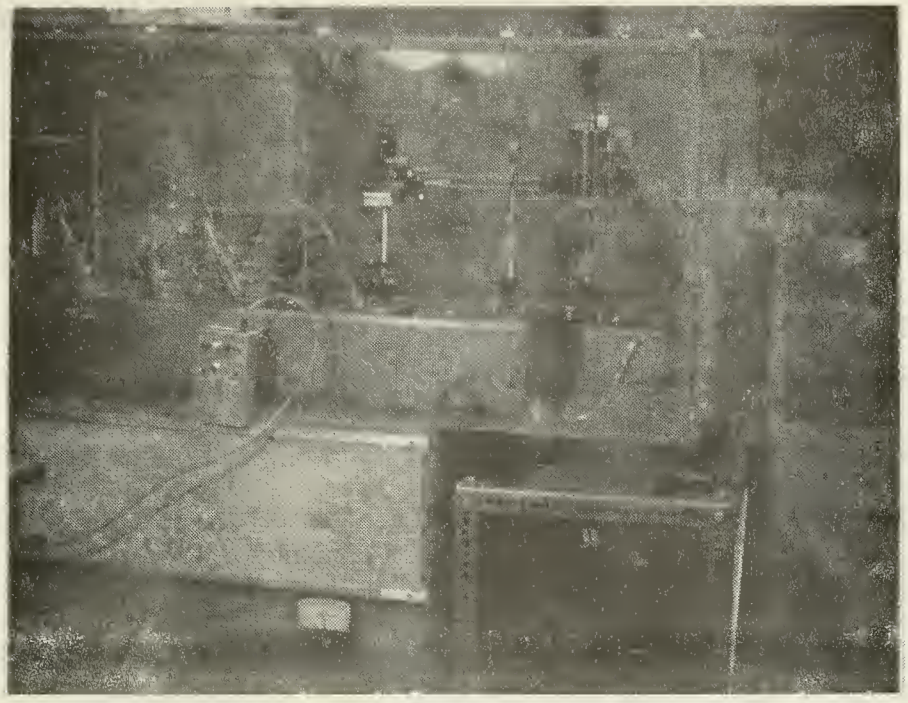

Figure 24. IR DETECTOR; CHARGING CONTROL BOX

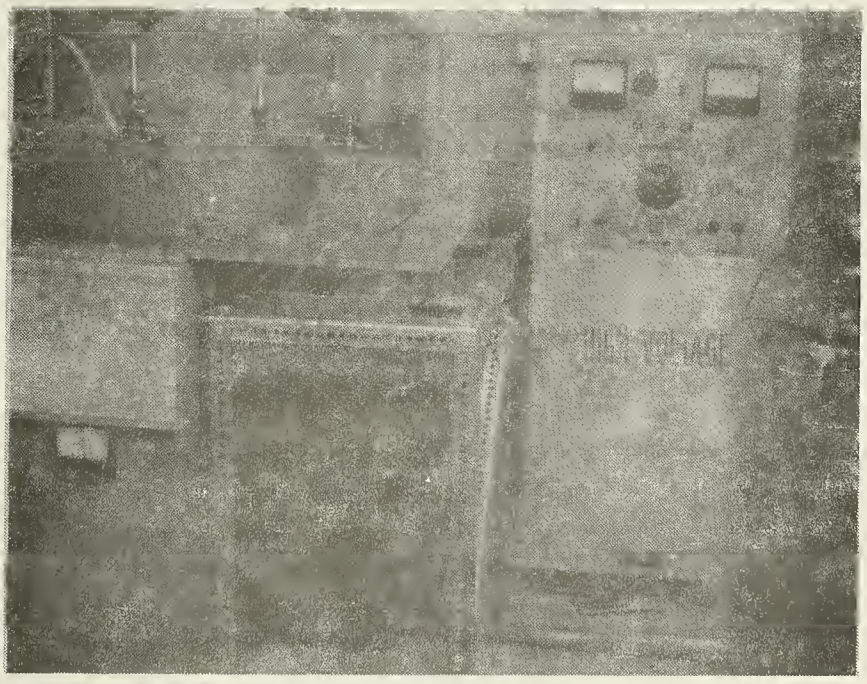

Figure 25. HIGH VOLTAGE POWER SUPPLY

APPENDIX F. INFRARED SPECTRA CALCULATIONS FOR DIATOMICS

A computer program [Ref. 12] in Basic was written to calculate and list the wave numbers and wavelengths of the P- and R- branch transitions of $\Delta v=1$ for diatomic molecules. It can be used for any diatomic molecule for which the Dunham spectroscopic constants or their equivalents are known. Reference 12 gives the complete derivation of the equations used in the computer program. Table 2 gives the relevant spectroscopic constants [Ref. 4] for AlO, CuO and InO. The program has been executed for AlO and a sample output included in this Appendix. To use the data in the computer program, the following terms are nearly equivalent.

$W_e \approx Y_{10}$	$B_e \approx Y_{01}$	$D_e \approx -Y_{02}$	$W_e Y_e \approx -Y_{30}$	$\gamma_e \approx Y_{21}$
$W_e x_e \approx -Y_{20}$	$\alpha_e \approx -Y_{11}$	$\beta_e \approx -Y12$	$W_e Z_e \approx -Y_{40}$	$\delta_e \approx -Y_{31}$

The data is entered into the program in matrix form.

510 DATA Y_{00}, Y_{10}, Y_{20}, Y_{30}, ... Y_{10}

520 DATA Y_{01}, Y_{11}, Y_{21}, ... Y_{11}

530 DATA Y_{02}, Y_{12}, ... Y_{12}

540 DATA Y_{03}, ... Y_{13}

. . .

5__ DATA Y_{0m}, ... Y_{1m}

All DATA lines in the matrix must have the same number of entries; use zero to fill spaces of unknown constants.

	B_e	D_e	W_e	W_eX_e	α_e	β_e	W_eY_e	W_eZ_e	γ_e	δ_e
AlO	.64148	1.08×10^{-6}	978.2	7.12	.00575					
CuO			628	3						
InO			703.09	3.71			-.285			

TABLE 2. Infrared Spectroscopic Constants

Computer Program for Infrared Spectra Calculations

```
100  REM DIATOMIC MOLECULAR SPECTRA
110  READ A,B
120  READ C,D
130  DIM Y(10,10)
140  FOR M=0 TO D
150  FOR L=0 TO C
160  READ Y(L+1,M+1)
170  NEXT L
180  NEXT M
190  FOR V=1 TO A
200  PRINT 'V=',V,'TO',V-1,'P- AND R-BRANCH TRANSITIONS FOR',
210  PRINT 'ALUMINUM OXIDE'
220  PRINT 'J OF P(J)','WAVE NO.','WAVELENGTH','J OF R(J)',
230  PRINT 'WAVE NO.','WAVELENGTH'
240  FOR J=1 TO  B
250  LET I=J-1
260  LET S1=0
270  LET S2=0
280  LET G=0
290  FOR L=0 TO C
300  LET G=G+Y(L+1,1)*((V+.5)**L-(V-.5)**L)
310  NEXT L
320  FOR L=0 TO C
330  FOR M=1 TO D
331  LET R=Y(L+1,M+1)
340  LET E=(V+.5)**L*(I+1)**M*(I+2)**M
350  LET S1=S1+R*((V+.5)**L*J**M*(J-1)**M-(V-.5)**L*J**M*(J+1)**M)
360  LET F=(V-.5)**L*I**M*(I+1)**M
370  LET S2=S2+Y(L+1,M+1)*(E-F)
380  NEXT M
390  NEXT L
400  LET S1=S1+G
410  LET S2=S2+G
420  PRINT J,S1,10000/S1,I,S2,10000/S2
430  NEXT J
440  PRINT
450  PRINT
460  PRINT
470  PRINT
480  NEXT V
490  DATA 10,25
500  DATA 2,4
510  DATA 0,978.2,-7.12
520  DATA .64148,.00575,0
530  DATA .00000108,0,0
540  DATA 0,0,0
550  DATA 0,0,0
999  END
```

J OF P(J)	WAVE NO.	WAVELENGTH	J OF R(J)	WAVE NO.	WAVELENGTH
1	962.671	10.3878	0	965.26	10.3599
2	961.394	10.4016	1	966.572	10.3458
3	960.128	10.4153	2	967.895	10.3317
4	958.874	10.4289	3	969.23	10.3175
5	957.631	10.4424	4	970.576	10.3032
6	956.399	10.4559	5	971.935	10.2888
7	955.179	10.4692	6	973.304	10.2743
8	953.97	10.4825	7	974.686	10.2597
9	952.772	10.4957	8	976.079	10.2451
10	951.586	10.5088	9	977.484	10.2303
11	950.411	10.5218	10	978.9	10.2155
12	949.247	10.5347	11	980.329	10.2007
13	948.094	10.5475	12	981.769	10.1857
14	946.953	10.5602	13	983.221	10.1707
15	945.822	10.5728	14	984.685	10.1555
16	944.703	10.5853	15	986.161	10.1403
17	943.595	10.5978	16	987.648	10.1251
18	942.497	10.6101	17	989.148	10.1097
19	941.411	10.6224	18	990.66	10.0943
20	940.336	10.6345	19	992.184	10.0788
21	939.272	10.6465	20	993.719	10.0632
22	938.219	10.6585	21	995.267	10.0476
23	937.177	10.6703	22	996.827	10.0318
24	936.145	10.6821	23	998.399	10.016
25	935.125	10.6938	24	999.983	10.0002

P- AND R-BRANCH TRANSITIONS FOR ALUMINUM OXIDE, V=1 to 0

J OF P(J)	WAVE NO.	WAVELENGTH	J OF R(J)	WAVE NO.	WAVELENGTH
1	948.419	10.5439	0	951.031	10.5149
2	947.131	10.5582	1	952.354	10.5003
3	945.853	10.5725	2	953.689	10.4856
4	944.587	10.5866	3	955.036	10.4708
5	943.333	10.6007	4	956.394	10.4559
6	942.09	10.6147	5	957.763	10.441
7	940.858	10.6286	6	959.145	10.426
8	939.638	10.6424	7	960.538	10.4108
9	938.428	10.6561	8	961.942	10.3956
10	937.231	10.6697	9	963.358	10.3804
11	936.044	10.6833	10	964.787	10.365
12	934.869	10.6967	11	966.227	10.3495
13	933.704	10.71	12	967.678	10.334
14	932.551	10.7233	13	969.142	10.3184
15	931.409	10.7364	14	970.617	10.3027
16	930.279	10.7495	15	972.104	10.287
17	929.159	10.7624	16	973.604	10.2711
18	928.05	10.7753	17	975.115	10.2552
19	926.952	10.788	18	976.638	10.2392
20	925.866	10.8007	19	978.173	10.2231
21	924.79	10.8133	20	979.72	10.207
22	923.726	10.8257	21	981.28	10.1908
23	922.672	10.8381	22	982.851	10.1745
24	921.629	10.8504	23	984.434	10.1581
25	920.597	10.8625	24	986.03	10.1417

P- AND R-BRANCH TRANSITIONS FOR ALUMINUM OXIDE, V=2 to 1

J OF P(J)	WAVE NO.	WAVELENGTH	J OF R(J)	WAVE NO.	WAVELENGTH
1	934.167	10.7047	0	936.302	10.6746
2	932.867	10.7196	1	938.137	10.0594
3	931.578	10.7345	2	939.483	10.6441
4	930.301	10.7492	3	940.841	10.6288
5	929.035	10.7639	4	942.21	10.6133
6	927.78	10.7784	5	943.592	10.5978
7	926.537	10.7929	6	944.984	10.5822
8	925.305	10.8072	7	946.389	10.5665
9	924.084	10.8215	8	947.805	10.5507
10	922.875	10.8357	9	949.233	10.5348
11	921.677	10.8498	10	950.672	10.5189
12	920.49	10.8638	11	952.124	10.5028
13	919.314	10.8777	12	953.587	10.4867
14	918.15	10.8915	13	955.062	10.4705
15	916.996	10.9052	14	956.549	10.4542
16	915.854	10.9188	15	958.048	10.4379
17	914.723	10.9323	16	959.558	10.4215
18	913.602	10.9457	17	961.082	10.4049
19	912.493	10.959	18	962.616	10.3884
20	911.395	10.9722	19	964.163	10.3717
21	910.308	10.9853	20	965.721	10.355
22	909.232	10.9983	21	967.292	10.3381
23	908.167	11.0112	22	968.875	10.3213
24	907.112	11.024	23	970.47	10.3043
25	906.069	11.0367	24	972.077	10.2873

P- AND R-BRANCH TRANSITIONS FOR ALUMINUM OXIDE, V=3 to 2

BIBLIOGRAPHY

1. Currie, C. L., Darwent, B. deB., "The Photochemical Decomposition of Methyl Azide," Canadian Journal of Chemistry, V. 41, 1963.

2. Chace, W. G., and Moore, H. K., Exploding Wires, V. 1-4, Plenum Press, 1968.

3. Dzhidzhoev, M. S., et al., "Creation of a Population Inversion in Polyatomic Molecules Through the Energy of Chemical Reactions," Soviet Physics JETP, V. 30-2, Feb. 1970.

4. Herzberg, G., Molecular Spectra and Molecular Structure I. Spectra of Diatomic Molecules, 2nd Ed., Van Nostrand Reinhold, 1950.

5. Houck, T. L., Pulsed Gain Measurements on CO_2 Lasers, Master's Thesis, U.S. Naval Postgraduate School, Monterey, California, 1971.

6. Jensen, R. J., Rice, W. W., "Chemical Lasers: A Light Review," Chemtech, April, 1972.

7. Levine, A. K., Lasers, V. 1 and 2, Marcel Dekker, Inc., 1966.

8. Levine, A. K., DeMaria, A. J., Lasers, V. 3, p. 111-269, Marcel Dekker, Inc., 1971.

9. O'Dell, M. S., Jr., Darwent, B. deB., "Thermal Decomposition of Methyl Azide," Canadian Journal of Chemistry, V. 48, No. 7, 1970.

10. Pimental, George C., "Infrared Study of Transient Molecules in Chemical Lasers," Pure and Applied Chemistry, V. 18, No. 3, p. 275-283, 1969.

11. Rice, W. W., and Jensen, R. J., "A Practical Chemical Laser System," Journal of Chemical Education, V. 48, p. 659-662, October, 1971.

12. Rice, W. W., and others, "Metal Atom Oxidation Lasers," Los Alamos Scientific Laboratory, March, 1974.

13. Rice, W. W., "Aluminum Fluoride Exploding Wire Laser," Appl. Phys. Lett., Vol. 22, No. 2, 15 Jan 1973.

14. Russel, G. R., and others, "Supersonic Electric-Discharge Copper-Vapor Laser," Appl. Phys. Lett., V. 21, No. 12, 15 Dec 1972.

15. Report by "Committee on New Gas 'Visible' Lasers," September, 1972.

16. Schnez, G. P., The CO_2-HN_3 Laser: Design and Construction of a Molecular Laser Pumped by Photolysis of HN_3, Master's Thesis, U.S. Naval Postgraduate School, Monterey, California, 1971.

17. Siegman, A. E., An Introduction to Lasers and Masers, Preliminary Edition, McGraw-Hill, 1968.

18. Silfvast, W. T., "Metal Vapor Lasers," Scientific American, Feb., 1973.

INITIAL DISTRIBUTION LIST

		No. Copies
1.	Defense Documentation Center Cameron Station Alexandria, Virginia 22314	12
2.	Library (Code 0212) Naval Postgraduate School Monterey, California 93940	2
3.	Commander Naval Air Systems Command Department of the Navy Washington, D.C. 20360	
	ATTN: AIR 310	2
	AIR 604	2
4.	Chairman Department of Aeronautics Naval Postgraduate School Monterey, California 93940	1
5.	Professor D. J. Collins Department of Aeronautics Code 57CO Naval Postgraduate School Monterey, California 93940	2
6.	Mr. L. S. McDonald Naval Air Systems Command Code AIR 3033 Department of the Navy Washington, D.C. 20360	1
7.	Dean of Research Naval Postgraduate School Monterey, California 93940	2
8.	Mr. J. W. Willis Naval Air Systems Command Code AIR 310B Department of the Navy Washington, D.C. 20360	1
9.	Dr. Walter W. Rice Los Alamos Scientific Laboratory Los Alamos, New Mexico 87544	1

10. Professor O. Biblarz 1
Department of Aeronautics
Code 57ZI
Naval Postgraduate School
Monterey, California 93940

11. LT Leslie G. Murray 1
SMC # 1321
Naval Postgraduate School
Monterey, California 93940

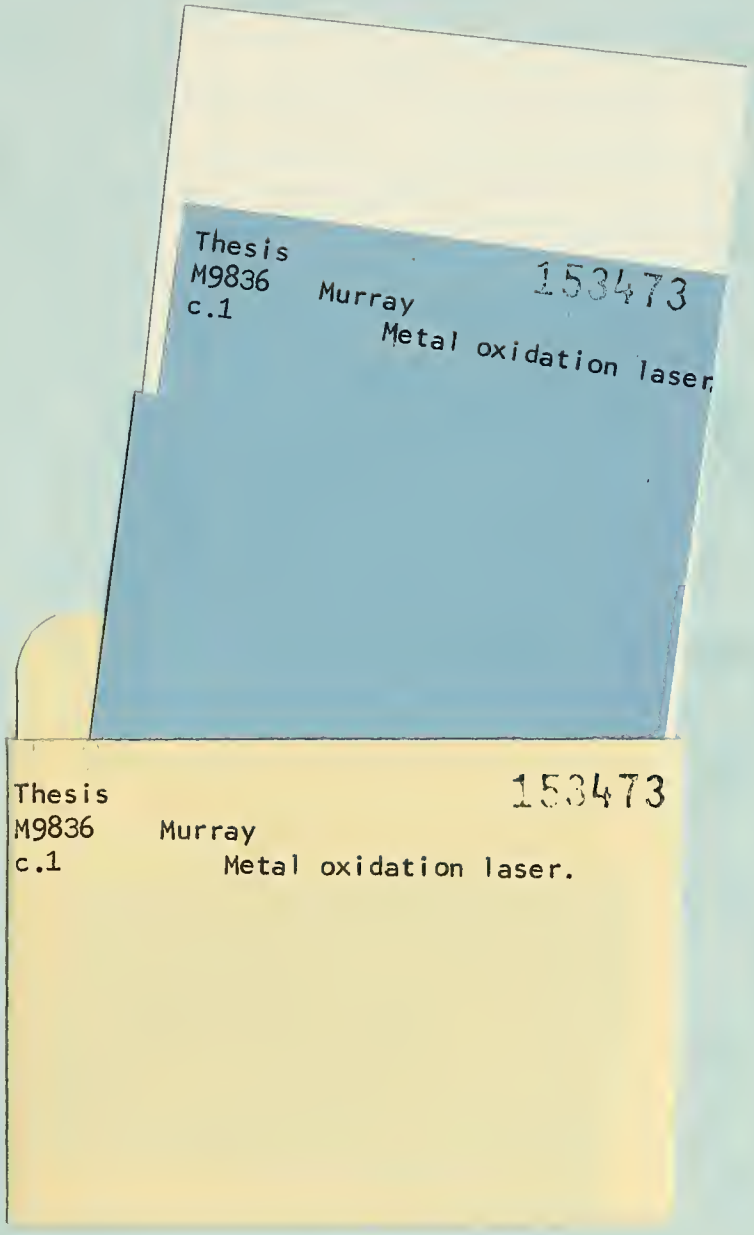

Thesis
M9836
c.1
Murray
153473
Metal oxidation laser.